Chemical modifications of AFM tips for the study of molecular recognition events

Régis Barattin[a] and Normand Voyer*[b]

Received (in Cambridge, UK) 2nd October 2006, Accepted 24th January 2008
First published as an Advance Article on the web 29th February 2008
DOI: 10.1039/b614328h

The use of AFM to study molecular recognition events at an incredible level of sensitivity is currently a very active field of research. In order to get information at the single molecule level, it is mandatory to modify in a precise manner the AFM tip to anchor either ligand or receptor molecules. In the following lines, we review the achievements in tip modifications and illustrate the scope and limitations of the different strategies that have been reported.

Introduction

Since its invention in 1986 by Binnig *et al.*,[1] atomic force microscope (AFM) has increasingly been used, not only to image surfaces of interest, but also to investigate mechanical forces and molecular interactions.

Because of its remarkable properties, including the option to operate under aqueous and physiological conditions, and its exceptionally high lateral sub-nanometer resolution, AFM has rapidly been developed to study biological processes[2] and for single molecule experiments.[3]

In recent years, there has been growing interest in studying single molecule recognition events using chemically-modified AFM tips. In general, the major hurdle for such studies is the lack of control of the probe modification step of the AFM tip, which affects the measurement of single molecular interactions.

In the following article, after a brief overview of various applications of AFM, we review achievements in the chemical modifications of AFM tips, and discuss possible improvements needed to allow the well defined functionalization of these tips.

[a] *CEA-LETI, Laboratoire de Fonctionnalisation et Chimie pour les Microsystèmes, 17 rue des Martyrs, F-38054 Grenoble cedex 9, France*
[b] *Centre de recherche sur la fonction, la structure, et l'ingénierie des protéines, Département de chimie, faculté des Sciences et de Génie, Université Laval, Québec, Canada G1K 7P4. E-mail: normand.voyer@chm.ulaval.ca; Fax: +1 (418) 656-7916; Tel: +1 (418) 656-3613*

1. The atomic force microscope

1.1 Apparatus

The principal set-up of AFM is shown in Fig. 1, and consists of a sharp tip integrated into the apex of a microfabricated cantilever spring, a solid substrate surface (piezo scanner) to support the sample, an optical beam apparatus to detect the cantilever's deflection, and an electronic system to record and analyze data.

Régis Barattin studied chemistry at the Joseph Fourier University of Grenoble, France, where he received his PhD in 2003. During a first postdoctoral position at the Laval University of Quebec, Canada, under the supervision of Professor Normand Voyer, he worked on the design and engineering of peptide nanostructures and on their grafting onto AFM tips for the study of molecular recognition events. In 2006, he joined the Nanosciences Group of the Center for Material Elaboration & Structural Studies (CEMES) in Toulouse, France, to work on the synthesis of molecular landers. Since 2007, he has worked at CEA-LETI in Grenoble, France, on the functionalization of silicon surfaces for molecular electronic applications.

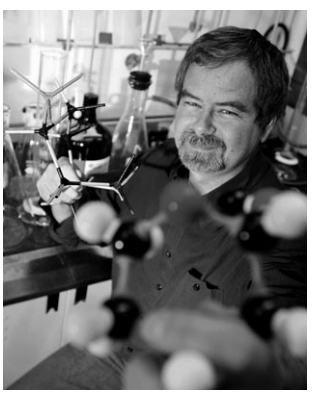

Normand Voyer studied chemistry at the Laval University of Quebec, Canada, where he received his PhD in 1985. After his postdoctoral work, carried out under the supervision of Professor Donald James Cram at UCLA, he joined, in 1988, the University of Sherbrooke, Canada, as Associate Professor. In 1996, he came back to the Laval University of Quebec, Canada, where he is still working as Full Professor of Bioorganic Chemistry. Since 1999, he has been Director of the Protein Function, Structure and Engineering Research Center, Quebec, Canada, and since 2005, he has also been Director of the Chemistry Department of the Laval University of Quebec, Canada. His research interests are the design, synthesis and characterization of protein and peptide-based supramolecular devices, as well as the development of artificial ion channels and synthetic carriers of biologically relevant compounds.

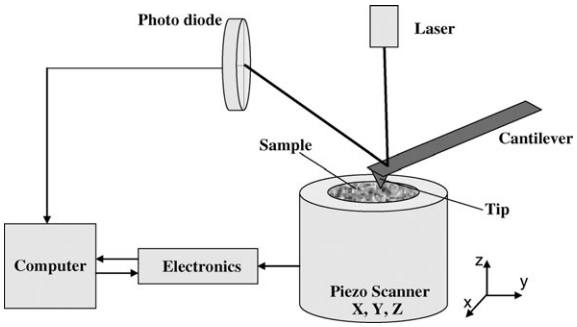

Fig. 1 Schematic drawing of an AFM apparatus.

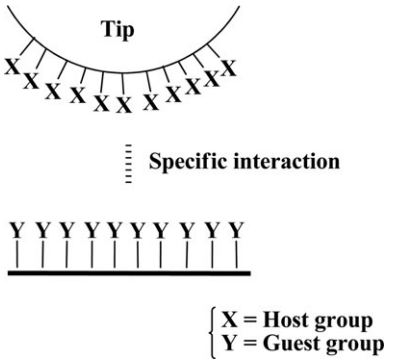

Fig. 2 Schematic drawing of a chemically-modified tip with functional groups X that provide a specific interaction with functional groups of interest Y on the sample surface.[19]

AFM probes the surface-supported sample by scanning the tip. The tip position, which reflects the tip–surface interaction, is monitored by the deflection of a laser beam on the cantilever, which is measured by a position-sensitive quadrant photodiode. The computer and electronic system then record cantilever position (Z) at each point of the scanned surface (X, Y).

Two basic modes of AFM are generally employed to investigate substrate surfaces. In contact mode, the tip remains in permanent contact with the sample and becomes very sensitive to each small change on the surface. On the other hand, in dynamic mode, the surface is scanned with the tip oscillating close to its resonant frequency. During the scan, the contact between the ''tapping'' probe and the surface results in a reduction of the cantilever vibration amplitude, which is monitored by laser deflection. Several intermittent contact modes are generally used. For example, in magnetic AC mode (MAC), the cantilever is driven directly by an alternative magnetic field.[4–6] In pulsed-force mode AFM (PFM-AFM), tapping is provided by bringing the sample and the AFM tip into contact and detaching them cyclically with a much lower frequency than the resonance frequencies of the cantilever and scanner.[7,8]

1.2 Imaging

One of the first applications of AFM was the imaging of surfaces, generally under atmospheric pressure, vacuum or gaseous conditions. The ability of AFM to image under aqueous conditions allows the investigation of a variety of biological systems.[9] For biomolecular imaging studies, both contact and tapping modes have been used.[10] Although contact mode provides higher resolution images, samples scanned must usually be immobilized straight onto a surface to avoid damage or deformation of the substrate. Alternatively, tapping mode reduces molecular motion and deformation, and therefore allows the study of isolated biological molecules under physiological conditions with better accuracy.

Several examples of high resolution biomolecular imaging with AFM have been described in the last 15 years.[6,10–15] These studies include images of not only single molecules (DNA and RNA) but also biological assemblies (biological membranes, membrane and non-menbrane proteins, cell surfaces, antibodies, viruses and bacteria), and images of tissues and organs. For most of these, a lateral resolution of 100 nm and a vertical resolution of 10 nm have been achieved.

In addition, progress in the application of AFM to imaging biomolecules in their native environment has made it possible to visualize biochemical processes, such as RNA transcription or the conformational changes of membrane proteins.[16,17]

1.3 Force microscopy

As was described previously, the use of AFM with bare tips allows topographical images of surfaces to be obtained. In Force Microscopy, probes are chemically modified to make them sensitive to a specific molecular interaction. In this way, it possible to measure probe–sample forces and to investigate chemically-sensitive imaging.

1.3.1 Chemical force microscopy. In Chemical Force Microscopy (CFM),[18] AFM tips are modified with specific chemical functional groups, as shown in Fig. 2, generally by the use of self-assembled monolayers (SAMs).[19–21] CFM measures the adhesion or friction forces between functional groups on probe tips (X) and the chemical functionality of interest (Y) bound to the surface by exploiting their specific interactions (such as hydrophobic–hydrophilic, hydrogen bonding, van der Waals, Coulombic interactions, π-stacking, *etc.*). This enables the modified tip to generate a contrast between regions containing different chemical functionalities, and then to map their spatial distribution on the surface.

1.3.2 Single molecular force recognition microscopy. Due to its force detection sensitivity, AFM also enables detection of specific interaction forces at the single molecule level. In so-called Single Molecular Force Recognition Microscopy (SMRFM), tips are functionalized with one or a few probe molecules that can recognize a specific type of target molecule supported on the surface. During this force measurement, the tip doesn't scan the sample, but is brought into contact with the surface and retracted.

A schematic diagram of a typical force measurement cycle is shown in Fig. 3. The AFM tip is moved towards the surface (A) and brought into contact with the sample (B). At the end of the approach motion, the tip is pressed onto the sample surface (C, maximum point of load). The tip is then retracted to reach the point of the maximum probe–sample adhesion force (D). During this retraction phase, forces applied to the tip are due to the interactions between the probe and the

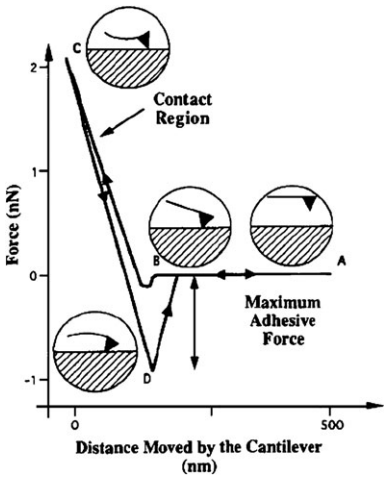

Fig. 3 Schematic diagram of a typical force–distance measurement cycle.[32]

sample. In this way, the cantilever deflection signal associated with the retracting force needed to withdraw the probe from the surface (from point D to A) is related directly to probe–sample adhesion force. The value of this force is then obtained using Hooke's Law ($F = -kd$), which converts the cantilever deflection (d) into the force F (pN range).†

SMRFM has been greatly employed to measure both intramolecular and intermolecular forces between single molecules. Several of these studies have been already reported in reviews.[3,22–24] In intramolecular force spectroscopy experiments, single molecules are tethered between the tip and a supporting surface. Upon retraction of the tip, the deflection of the cantilever reflects the mechanical properties of the studied macromolecule. For instance, conformational dynamics, elasticity and stretching of peptides,[25–27] polymers[28–30] or DNA duplexes[31] can be estimated.

On the contrary, in intermolecular force spectroscopy experiments, AFM has been employed to investigate a wide variety of single receptor–ligand binding phenomena. Biological ligands are anchored to the AFM tip and their corresponding binding partners (receptor) are supported on the surface, or *vice versa*. The measurement of force–distance cycles then allows the estimation of specific biological recognition forces.

Various examples of the determination of intermolecular interactions by single molecule force spectroscopy will be discussed later in this review.

In summary, AFM is a powerful method for imaging surfaces and biological systems, as well as for measuring the interaction forces of receptor–ligand pairs at the single molecule level. However, to obtain significant and reliable results on single molecule recognition events, it is mandatory to functionalize tips with a well-defined number of probe molecules. Furthermore, immobilization of the probe ligands on tips has to be strong enough to withstand the investigated receptor–ligand binding force and properly achieved so as to avoid interference with the recognition process under investigation.

† k is the cantilever spring constant.

As a result, the well-defined chemical modification of AFM tips is one of the most important features for obtaining successful data in molecular recognition event studies. In the following sections, we review the chemical modifications of tips reported to date in regards to the proper fixation of probe molecules.

2. Tip modifications

The choice of AFM tip is very important because it has a direct effect on the resolution of the image and on the accuracy of the measurement. Accordingly, several studies have been undertaken to improve tip parameters, such as shape apex, radius of curvature and cone angle, in order to enhance AFM tip efficiency.

2.1 AFM tips

Commercially available AFM tips consist of microfabricated pyramids of silicon (Si) or silicon nitride (Si_3N_4). Radii of curvature at the apex vary from 5–10 nm for silicon tips to 20–60 nm for Si_3N_4 tips, and the half cone angle is about 35° (Fig. 4a). Such characteristics will generally limit the effectiveness of imaging and constrain the lateral resolution. Sharper silicon tips can be fabricated[33] with improved geometrical factors (radius curvature as small as 2–5 nm and a half cone angle of about 10°), but the brittleness of such fine tips limits their stability and utility for conventional use (Fig. 4b).

To overcome these problems, different methods have been developed to create tips with enhanced properties. Silicon tips can be oxide-sharpened to improve their aspect ratio and reduce tip radius.[35] Sharper tips can also be manufactured by growing a carbon microtip at the apex of the tip, using electron beam deposition,[36,37] or a combination of focused ion and electron beam techniques.[38] With these methods, tips with high aspect ratios and radii curvatures as small as 5 nm can be obtained.

2.2 Tip coating

Despite the various methods described above, there remain important limitations. Indeed, the surfaces of most commercially available silicon-based tips are poorly controlled and may carry a large number of silanol groups. Such hydrophilic surfaces may be altered by the adsorption of contaminants and may also cause damage to hydrophilic surface samples, such as proteins.[39] Moreover, such bare tips may change shape because of wear under prolonged usage. Therefore, tips have to be coated to avoid these important drawbacks.

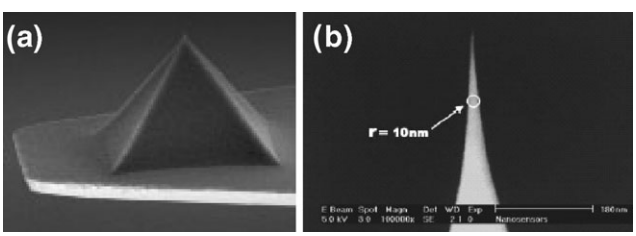

Fig. 4 SEM images of tips: (a) a silicon tip[34] and (b) a sharper silicon tip.[33]

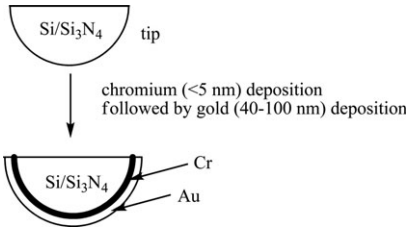

Fig. 5 General scheme for gold-coating.[39]

Coating methods consist of altering the surface composition of the tip to improve its properties, and to enhance imaging and force measurement capabilities. Amongst the methods known to coat AFM tips, the most currently used is gold-coating.

As shown in Fig. 5, the coating of silicon-based tips is a two-step process. A thin chromium adhesive layer is deposited (<5 nm), which is followed by the vapor deposition of a thicker gold layer (40–100 nm, or less). The initial chromium layer is necessary to ensure proper adhesion of the gold surface to the silicon or silicon nitride surface.[40] The major drawback of this coating technique is the loss of tip accuracy by the deposition of successive metal layers.

Other coatings with hollow metal tips, such as tungsten[35] or chromium,[41] have also been described, but the utilization of such tips is much less common. Similarly, a process for coating tips with nanocrystalline diamond by chemical vapor deposition has been developed, but only a few results have been reported with those tips, essentially for conducting AFM, topographical imaging or scanning probe microscopy.[42,43]

After the initial modification of tips, further functionalization has to be done on the surface to make the tip specific to target samples. As we will describe in the next section, both silicon-based tips and gold-coated tips can be used to obtain AFM molecular probes.

3. Tip surface chemical functionalization

In this section, we review the different ways to chemical functionalize AFM tips. From the perspective of settling single molecule recognition experiments, focus will be placed on how people have tried to functionalize a tip with only one molecule probe.

3.1 Functionalization with macromolecules

3.1.1 BSA adhesion on silicon tips. Florin *et al.* were the first, in 1994, to functionalize AFM tips to measure the specific interaction between biotin and avidin.[44,45] This receptor–ligand pair was chosen as a model system by virtue of its high specificity and affinity ($K_d = 10^{-15}$ mol L^{-1}), its well-known structural data,[46] and its broad range of applications.

Studies of adhesion forces in this system were performed by "tapping" a silicon tip functionalized with avidin, *via* biotinylated bovine serum albumin (BSA), onto a biotinylated agarose bead surface (Fig. 6a).

Other examples can also be found using biotin–BSA adsorption on a silicon tip for the study of biomolecular interactions.[32,47] Measurements of antibody–G protein interactions

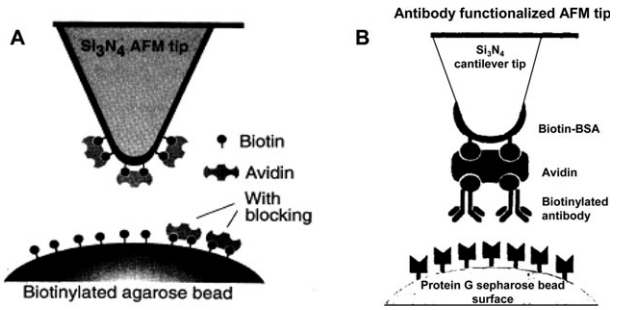

Fig. 6 Schematics of the biotinylated BSA functionalized tip. (a) Avidin functionalized AFM tip[44] (b) Antibody functionalized AFM tip.[45]

have also been investigated by coupling a biotinylated antibody to the tip *via* the avidin–biotin–BSA system (Fig. 6b).[45]

Functionalization of the AFM tip was undertaken by the adsorption of biotinylated BSA (biotin-BSA) onto the silicon nitride surface.[48] This adsorption process consisted of the overnight incubation of the tip in a biotin–BSA solution in a phosphate buffer saline solution (PBS).

According to the authors, the binding energy of biotin–BSA on the tip surface was strong enough (about -200 kJ mol^{-1}) to avoid the desorption of the BSA film during the biotin–avidin unbinding force (estimated at 88 kJ mol^{-1}) measurement.

The coupling of avidin to the tip *via* biotin–BSA was then undertaken by incubating the tip in an avidin solution in PBS for 5 min. During this step, it is likely that the tetrameric avidin molecule is attached to the tip *via* two or even three biotin binding sites. This way, it was assumed that no unbinding event between avidin and biotin–BSA should occur during the tip adhesion onto the biotinylated surface.

Nevertheless, a major drawback of this system is the lack of accuracy of the functionalized tip. As a matter of fact, the authors reported that during a force–distance measurement cycle, the interaction between the AFM tip and the bead involved as many as 100 biotin–avidin pairs. They have consequently proposed reducing the interaction area (by using smaller tips) and by decreasing the number of binding partners (by diluting the incubation solutions).

3.1.2 Electrografting polymers onto a gold tip. Jérôme *et al.* have recently reported a novel way of modifying AFM tips with a chemisorbed polymer.[49] This method is based on the approach of chemically grafting polymer films onto a metal surface by electropolymerization, as first described by Lécayon and co-workers.[50] According to this method, (meth)acrylic monomers can be electropolymerized by voltammetry at a well-defined cathodic potential.

This way, *N*-succinimidyl acrylate (NSA) was electrografted onto various conducting substrates, including gold, in DMF containing tetraethylammonium perchlorate as the conducting salt.[49] The mechanism of this process is illustrated in Fig. 7, and firstly involves the transfer of one electron from the metal to the monomer, which initiates the polymerization of the pre-absorbed monomer. Chain propagation then proceeds independently of any electrochemical reaction.

This technique was used to functionalize gold-coated AFM tips.[51] Force–distance measurements have been recorded

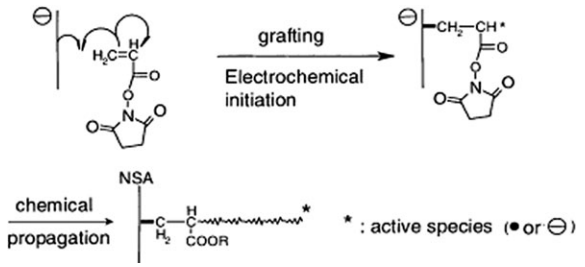

Fig. 7 Electrografting process of NSA.[51]

during approach–retraction cycles between the poly(*N*-succinimidyl acrylate) (PNSA)-coated tip and a bare silicon surface (Fig. 8), permitting adhesion forces (van der Waals and hydrogen bonding) between the PNSA coil and the silicon substrate to be determined (Fig. 8-1), as well as the intramolecular characteristics of polymer segments bridging the tip and silicon surface (Fig. 8-2).

To conclude, this electrografting method allows the functionalization of AFM tips with a strongly adhering polymer layer. The use of various (meth)acrylic monomers may open the way to further derivatization, as well as the anchoring of a wide variety of biological ligands onto the activated carboxylic groups.

Despite the efficiency of these methods in functionalizing tips *via* BSA adsorption or *via* an electrografting process, determination of the number of attached molecules on the tip could not be done exactly. To conclude, use of these inaccurate macromolecule-functionalizing systems might not be the most adequate strategy for studying single molecule recognition events.

3.2 Functionalization of AFM tips with Self-Assembled Monolayers (SAMs)

Another well-described functionalization route is based on the formation of self-assembled monolayers on the AFM tip surface.

3.2.1 Formation of SAMs on silicon tips. The chemical functionalizations of silicon tips described below are based on the well-known modifications of silicon surfaces. They rely on the chemical reaction of functional groups on the surface of the silicon tip with a variety of compounds to form covalent bonds.

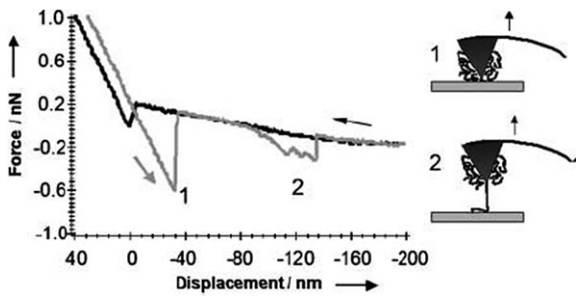

Fig. 8 Force–distance curves recorded between a polymer-grafted tip and a bare silicon substrate.[51]

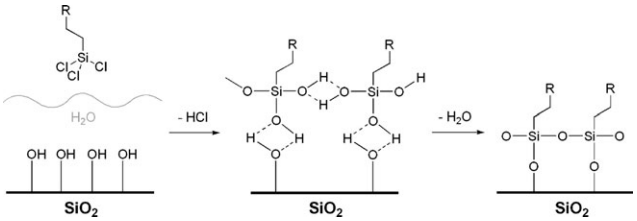

Fig. 9 Schematic representation of the silanization reaction process.[52]

3.2.1.1 Via *Si–O–Si bonds*. This first method is a silanization reaction based on the grafting of aliphatic chains onto the silica surface, *via* trichlorosilane groups, to form organosilane layers. The commonly assumed mechanism for this reaction has three steps (Fig. 9).[52]

First, the aliphatic chains are physisorbed onto the hydrated silica surface (carrying silanol groups) *via* the trichlorosilane groups. When the trichlorosilane groups get close enough to the surface, they are hydrolyzed. As a result, the aliphatic chains become bonded *via* hydrogen bonds to the surface silanols and to their close neighbors. After water elimination, the aliphatic chains are anchored to the silica surface *via* Si–O–Si covalent bonds to form polysiloxane monolayers.

This strategy has been widely applied to functionalize silicon-based tips. Prior to the reaction, silicon tip surfaces have to be activated to generate more surface hydroxyl groups. This activation is generally done by removing organic contaminants on the hydrophilic surface. Washing with Piranha solution (H_2SO_4/30% H_2O_2, 7 : 3) or with a 10% nitric acid solution, as well as by an ozone treatment followed by washing with alkaline and acid solutions, are usually sufficient.[53,54] Recently, Li *et al.* also reported a washing with 10% nitric acid solution followed by treatment in a silicone bath.[55] Surface-generated silanol groups, alkyltrichlorosilanes or alkyltrialkoxysilanes are directly coupled to form organosilane layers on the AFM tip (Fig. 10).

Modifications of organosilane SAMs can also be made after their formation on the tip. For instance, Ito *et al.*[53] have described the conversion of tip-supported vinyl-terminated SAMs to hydroxyl-terminated SAMs by hydroboration (Fig. 11).[56,57]

Another interesting tip modification by silanization is the incorporation of amino-terminated monolayers on the silicon

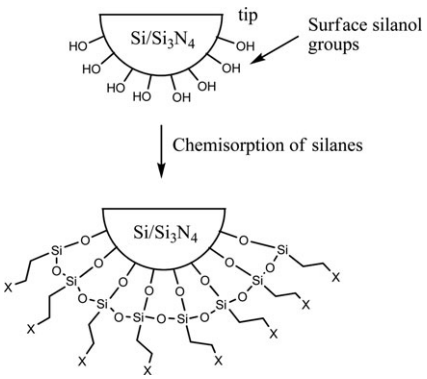

Fig. 10 Application of the silanization reaction to AFM tips. X represents different terminal groups.[39]

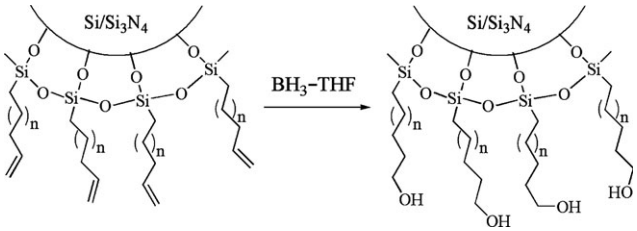

Fig. 11 Chemical modification of tip-supported vinyl-terminated SAMs by hydroboration.[53]

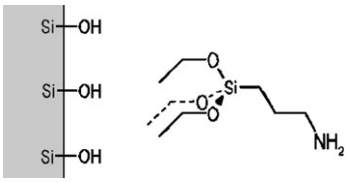

Fig. 12 Silanization with APTES.[58]

surface by reaction with 3-aminopropyl triethoxysilane (APTES), as illustrated in Fig. 12.[58]

These terminal amino functions have been used to anchor various biological probe ligands, such as antigen[59] or antibody,[55] to study binding forces between antigen and antibody by AFM.

Similarly, Vinckier *et al.* have developed a multi-step procedure, including the chemical modification of a supported alkyl silane, that allows the immobilization of proteins on the silicon surface.[60] The overall reaction scheme of this method is described in Fig. 13 (left). The first step is the coupling of an amino-terminated alkyl monoalkoxysilane with surface silanol groups, as described earlier. In the second step, the terminal amino group reacts with glutaraldehyde to form a reactive aldehyde functionality, linked through an imine bond. The protein is finally captured on the silicon surface *via* the formation of a second imine bond between an amino group on the surface of the protein and the terminal aldehydic group of the silicon-supported SAMs.

This strategy was later applied by Allen *et al.* to immobilize ferritin on an AFM probe, in order to monitor specific interactions between ferritin and antiferritin antibody (Fig. 13, right).[61]

The functionalization of silicon-based tips by the formation of organosilane SAMs is therefore a convenient way to change the surface chemistry of a tip and a valuable complement to

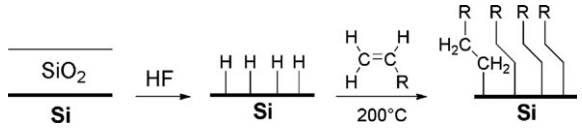

Fig. 14 General scheme for hydrosilylation modification of silicon tips.[64]

the metallization strategy. However, this silanization process presents several disadvantages. Because trichlorosilanes and trialkoxysilanes are very sensitive to moisture, they may be hydrolyzed before they are physisorbed on the silicon surface (Fig. 9). Moreover, difficulties remain in controlling the polymerisation process of the alkyl silane during the hydrolysis step at the surface.[62] Finally, the number of silanol groups cannot be estimated. These three points make it very difficult to find out precisely the thickness and composition of the alkyl silane film on the surface of the tip.

Consequently, because of the lack of control of the number of target molecules at the end of the tip-supported SAMs, this method is less appropriate for the study of single molecule force interactions.

3.2.1.2 Via *Si–C bonds: hydrosilylation*. Hydrosilylation is another approach to modify AFM tips that is based on the reaction of 1-alkenes with hydrogen-terminated silicon surfaces to form strong Si–C bonds (Fig. 14).[63]

The silicon surface has to be first etched by cleaning with Piranha solution (H_2SO_4/30% H_2O_2, 7 : 3) to remove organic contaminants, followed by removal of the oxide layer with HF in order to generate a hydrogen-terminated silicon surface.

Insertion of the unsaturated bond into the resulting silicon–hydride group can then be achieved by following one of two strategies. The first involves a thermally-induced hydrosilylation performed by immersion of the etched silicon surface into refluxing solutions of the appropriate 1-alkene (Fig. 14).[64] This reaction seems to be initiated by thermal homolytic Si–H bond cleavage, yielding the silicon surface-based radical, which can then react *via* the mechanism outlined in Fig. 15b. The second pathway uses a radical initiation step with diacyl peroxides, and the mechanism is also described in Fig. 15.[63,65]

In both of methods, the silicon surface is modified with dense and well-ordered alkane monolayers *via* very stable covalent Si–C bonds.

This hydrosilylation method has recently been applied to functionalize silicon AFM tips with an oligo(ethylene glycol) (OEG) derivative.[66] Direct chemisorption of OEG-alkenes

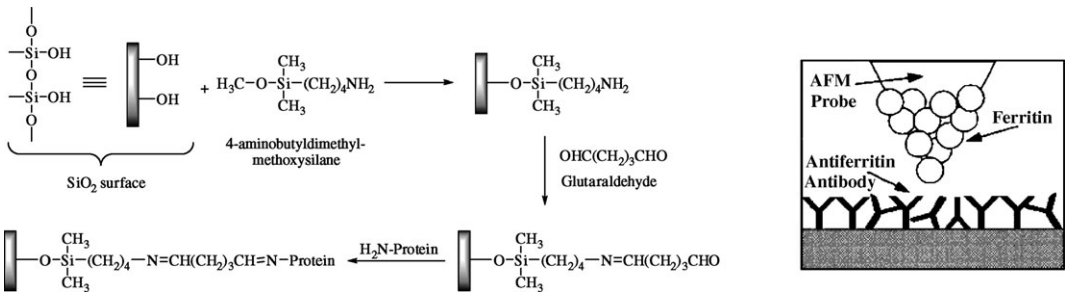

Fig. 13 Left: Overall reaction scheme for protein immobilization by the method of Vinckier *et al.*[60] Right: System developed to measure ferritin and antiferritin antibody interactions by AFM.[61]

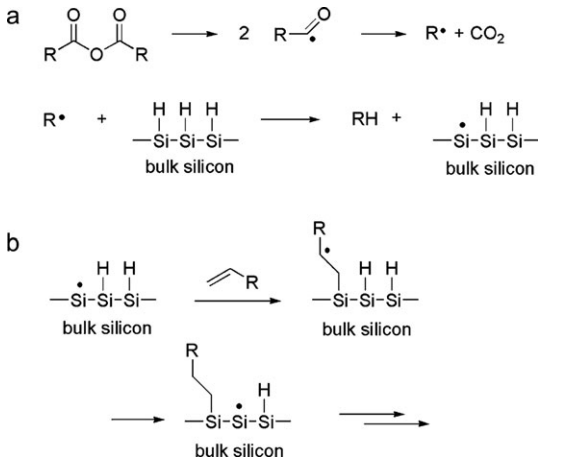

Fig. 15 Mechanism for radical-based hydrosilylation using diacylperoxides as initiators.[63]

onto a hydrogen-terminated silicon tip was done by thermal initiation, according to the process described above, to provide OEG monolayers (Fig. 16). This modified tip has been used to probe the interactions between the tip and films of fibrinogen and bovine serum albumin. It was shown that the OEG layer reduced the non-specific interaction of proteins compared to the bare tip while maintaining the capability for high resolution imaging.

Finally, hydrosilylation constitutes an interesting technique to coat silicon tips with robust monolayers of functional molecules. However, its use may be limited to chemical force microscopy or imaging spectroscopy as anchoring only one or very few functional molecules at the apex of AFM tip, a requirement for single molecule experiments, appears to be unachievable at present.

Despite the different methods we have described for modifying silicon AFM tips, only few examples are reported in the literature. The most used tip functionalization method is the chemisorption of thiols onto gold-coated tips.

3.2.2 Formation of SAMs on gold tips. The most popular approach to modify AFM tips is through the immobilization of thiol-based monolayers on gold-coated tips, as illustrated in Fig. 17.

The utility of thiols absorbed on gold as a monolayer system is based on three considerations. Firstly, gold is a relatively inert metal, it does not have a stable surface oxide and therefore it can be cleaned simply by removing physically and chemically adsorbed contaminants. Secondly, gold has a strong specific interaction with sulfur that permits the formation of stable monolayers. Thirdly, long chain alkane thiols

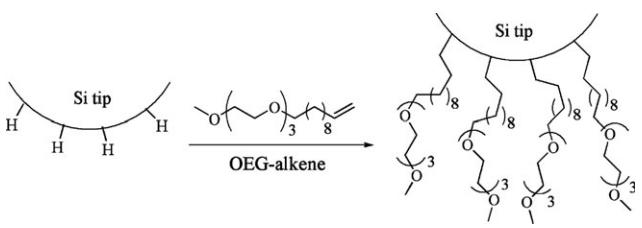

Fig. 16 OEG-modified AFM silicon tip by the hydrosilylation procedure.

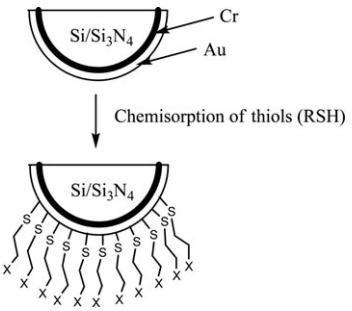

Fig. 17 Tip modification by formation of thiol-based monolayers on gold-coated tips.[39]

form a densely packed, crystalline or liquid-crystalline monolayer on gold.[67]

The reaction of alkane thiols adsorption onto a gold surface may be considered as an oxidative addition of the S–H bond to the gold surface, followed by a reductive elimination of hydrogen, as depicted below:

$$R\text{–}S\text{–}H + Au^0{}_n \rightarrow R\text{–}S^- Au^+ \cdot Au^0{}_n + \tfrac{1}{2}H_2$$

Consequently, the species formed are gold(I) thiolates ($RS^- Au^+$) adsorbed onto the gold(0) surface. The homolytic bond strength of the thiolate group at the gold surface is approximately 40 kcal mol^{-1}. Moreover, Skulason and Frisbies have estimated that the rupture force of a S–Au linkage is in the order of 10 kJ mol^{-1}, and have assigned it to the abstraction of thiolated, complexed Au atoms from the gold surface.[68] All of these data show that this bonding is very strong, and that the desorption of organosulfurs from the gold surface is very slow.[62]

From a practical point of view, thiol-based monolayers are obtained by the immersion of cleaned gold surfaces into thiol solutions for several hours. The solvent generally used is ethanol, but may vary according to the solubility of the alkane thiol used. Studies have shown that two distinct adsorption kinetics can be observed: a very fast step, by the end of which an imperfect monolayer is adsorbed, and a slower process of additional adsorption and consolidation, involving the displacement of contaminants, the expulsion of included solvent, and the lateral diffusion on the surface to reduce defects and enhancing packing.[67]

3.2.3 Examples of SAMs in CFM experiments. Few applications of SAMs on silicon and gold tips in CFM experiments have been reported.

For instance, Wenzler *et al*. have modified both SiO_2-coated AFM tips and glass surfaces with bromine- and methyl-terminated alkyltrimethoxysilane SAMs to probe specific chemical interactions (van der Waals and hydrophobic interactions) between the modified tip and a surface.[69]

As described below for silicon-based monolayers, thiol-based SAMs have been attached to AFM tips to study the interaction and spatial mapping of chemically-distinct functional groups by CFM. The measurement of adhesion and friction forces between two functionalized organic monolayers, respectively, on the AFM tip and sample surface has

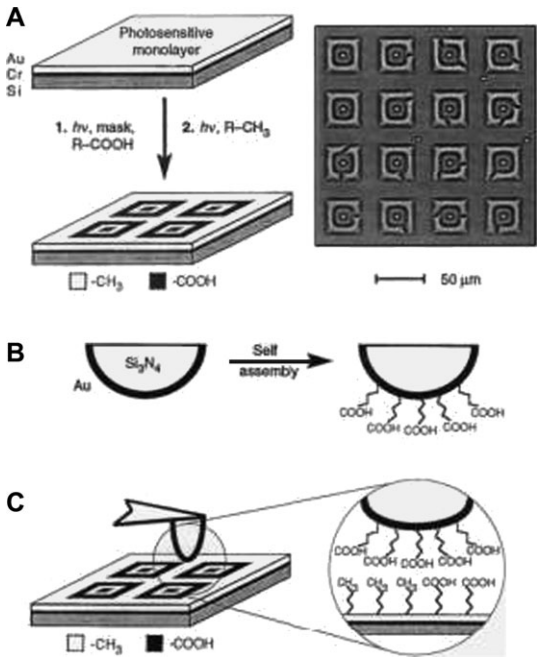

Fig. 18 Measurement of adhesive and friction forces by CFM between molecularly-modified probe tips and organic monolayer-terminating patterned samples.[70] A: Preparation of patterned sample surfaces containing lithographically-defined hydrophilic and hydrophobic regions. B: AFM tip modification with SAMs. The specific case of a tip terminated with COOH groups is shown. C: CFM experiment; interactions between a COOH-terminated tip and a patterned sample terminating in both CH_3 and COOH groups.

made it possible to produce a two-dimensional geometrical distribution of distinct functional groups.

Lieber *et al.* were the first to report this kind of experiment.[20,21,70] In a typical experiment, a gold-coated probe tip can be functionalized with either CH_3- or COOH-terminated SAMs. Surfaces have been lithographically patterned with defined hydrophilic (COOH) and hydrophobic (CH_3) regions, as illustrated in Fig. 18A. Then, the gold tip can be modified by forming a SAM using an alkane thiol with a carboxylic acid end group (Fig. 18B).

The adhesive forces between tip and surface can be measured (Fig. 18C). It has been shown that the interaction between hydrophilic groups, which can form hydrogen bonds, is stronger than between hydrophobic groups. These phenomena have made it possible to identify the different functional groups (–COOH and $–CH_3$) simply on the basis of the magnitude of the measured adhesive force and allowed the spatial mapping of friction forces between the functionalized tip and lithographically-patterned samples (Fig. 19).

Topographic and lateral force images have been recorded with both CH_3- and COOH-functionalized tips on surfaces terminated with CH_3 and COOH groups. When a CH_3-terminated tip was used for imaging, the CH_3-terminated regions of the sample exhibited a larger friction than the COOH-terminated regions (Fig. 19B), while no discrimination could be identified from topographical images recorded with a bare tip. When a COOH-terminated tip was used, the friction contrast was reversed (Fig. 19C).

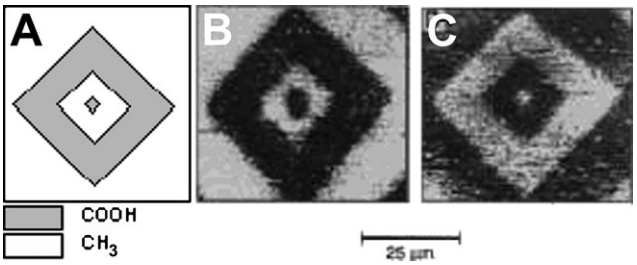

Fig. 19 Spatial mapping of friction forces between molecularly-modified probe tips and organic monolayer-patterned samples.[70] (a) Representation of CH_3- and COOH-terminated regions of the sample. (b) Image of the friction force recorded with a CH_3-terminated tip. The bright regions correspond to a high friction force. (c) Image of the friction force recorded with a COOH-terminated tip.

In that example, hydrogen bonding, dipole–dipole interactions and hydrophobic interactions were all involved, allowing discrimination between these two different chemical functionalities. Other examples involving electrostatic interactions have been reported, and have shown that it is also possible to map the distribution of charged groups.

For example, Hadziioannou and van der Vegte modified an AFM tip and a sample surface with COOH and NH_2-terminated alkane thiol monolayers, and studied the chemical-specific tip–surface interactions as a function of pH.[19,71] According to changes in the ionization of both chemical functionalities when the pH of the medium was changed (Fig. 20), measurement of the resulting adhesion and friction forces enabled the differentiation of surface-bound functional groups, providing chemical-specific imaging.

These studies show that the use of alkane thiol-based monolayers to modify AFM tips is very helpful for mapping the spatial arrangement of chemical functional groups on a surface by measuring adhesive and friction forces with a conveniently functionalized tip. However, it is important to recognize that the measured forces correspond to interactions between several functional groups. For example, Lieber *et al.* have estimated that the measured force results from interactions between around 50 functional groups on the sample and tip.[70]

3.2.4 Examples of SAMs in SMRFM experiments. As well as for CFM experiments, several examples of the use of SAMs have been reported for the study of molecular force recognition.

Fig. 21 shows examples of modified silanes, carrying target molecules, used to form SAMs on AFM tips. An alkyl silane derivative with an 18-crown-6 moiety (Fig. 21a) has been grafted onto an AFM tip to measure the intermolecular forces of complexation between a crown ether fixed on the tip and

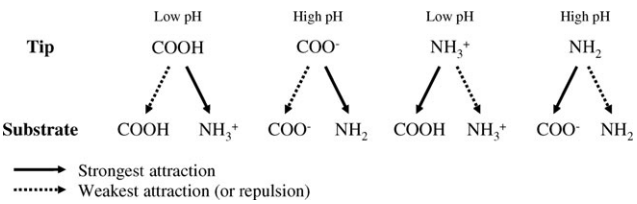

Fig. 20 Changes in friction forces according to pH.[19]

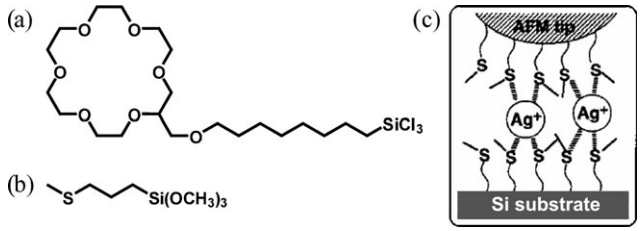

Fig. 21 Examples of silanization reagents. (a) Alkyl silane derivative with an 18-crown-6 moiety,[72] (b) [3-(methylthio)propyl]trimethoxysilane and (c) proposed mode of action of an AFM tip modified with the latter for measuring binding forces between silver ions and thioethers.[54]

guest ions (K^+, Li^+, *etc.*) in solution.[72] [3-(Methylthio)propyl]trimethoxysilane (Fig. 21b) has also been used to form methylsulfanyl-terminated SAMs on AFM tips and silicon surfaces in order to study the binding of ionic species (Ag^+, H^+) by adhesion force measurements between tip and surface (Fig. 21c).[54]

The silanization reaction has also been used to functionalize a silicon nitride tip with an electron deficient trinitrofluorenone derivative (Fig. 22). Such a tip was used to measure the binding force of charge transfer complexes formed between the electron deficient moiety and an electron-rich 9-anthracene methanol derivative linked to a glass surface (Fig. 22).[73]

In addition to the functionalization of silicon tips with SAMs, the formation of alkane thiol-based SAMs with peptides on gold tips has been also been reported recently.[74] A peptide with the amino acid sequence His–Ala–Ser–Tyr–Ser (HASYS) was modified at the *C*-terminus with a cysteine, which allowed its anchoring onto a gold-coated tip surface (Fig. 23). The experimental preparation of the peptide monolayer followed the general procedure described for other alkane thiols.

Functionalization of the tip and sample surface with the same peptide monolayers was used to investigate the interaction between a cationic porphyrin (TMpyP) (Fig. 23a) and the peptide HASYSC using AFM (Fig. 23b). Binding interactions between these two partners involved π-electron stacking be-

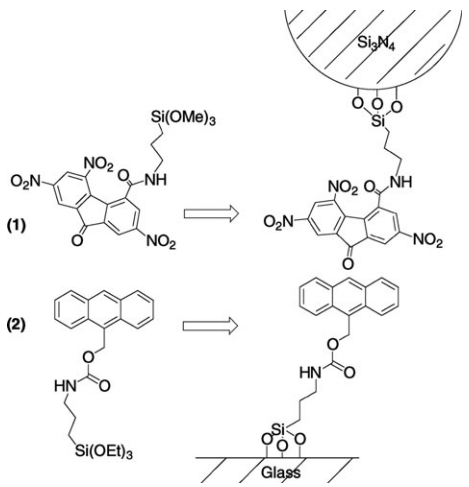

Fig. 22 Representation of a modified tip to measure forces of charge transfer complexes.[73]

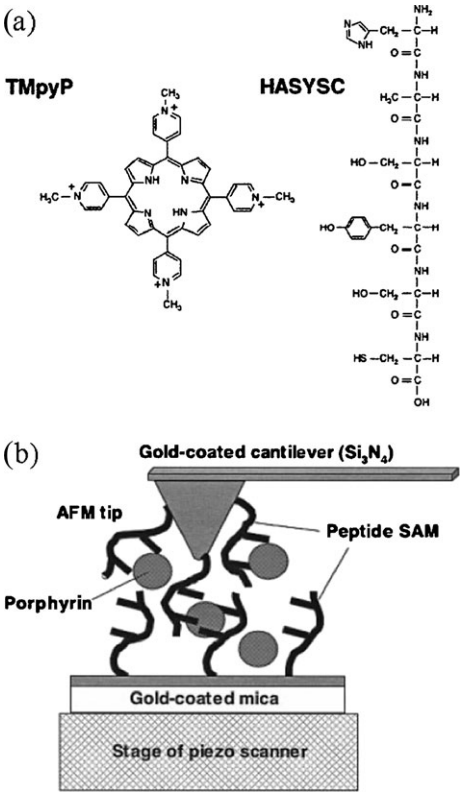

Fig. 23 Formation of peptide-terminated SAMs for the determination of porphyrin–peptide binding forces.[74] (a) Chemical structure of the porphyrin (TMpyP) and peptide (HASYSC). (b) Schematic of the AFM experiment.

tween the side chains of histidine and tyrosine, and the porphyrin. Nakamura *et al.* found that the porphyrin interacted with at least two peptides, and estimated by force distance experiments the unbinding force of the porphyrin–peptide complex.

Nevertheless, this system does not seem able to determine precisely and directly the force required for the unbinding of a single porphyrin–peptide complex. This is mainly due to the large number of peptide chains on the tip and substrate, and the lack of information on the number of peptides that contribute to the binding of one porphyrin.

In all of these cases, adhesive contacts between the tip and the substrate are made and broken multiple times. These consecutive pull-off measurements gave rise to a distribution of forces, plotted as a histogram of pull-off forces. This distribution can be analyzed to determine the force associated with the rupture of a single chemical bond. In this way, the approach allows the detection of single bond forces amongst multiple bond forces.

Moreover, trying to solve the problem of detecting single bond forces in AFM pull-off measurements, Skulason and Frisbie used a modified Johnson–Kendall–Roberts (JKR) contact mechanics model and concluded that stringent requirements for the tip were necessary, such as substrate interfacial energy, tip radius and bond formation probability.[75] Using this approach, they measured the chemical binding force of discrete electron donor complexes formed at the interface between proximal SAMs (Fig. 24).[76]

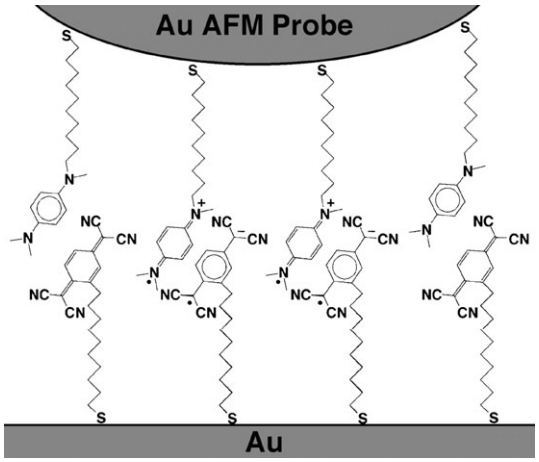

Fig. 24 Schematic representation of charge transfer complex formation for the direct detection of single bond forces by AFM.[76]

The examples described above show that functionalization of a tip with a dense SAM of molecular probes needs to be investigated by further analysis in order to discriminate single bond forces from among the multiple measured forces. One way to circumvent this approach is to reduce the number of ligands of interest on the tip in order to make sure that only one binding complex is involved in the force measurement. This has been achieved by preparing mixed SAMs.

3.2.5 Formation of mixed SAMs. The preparation of mixed SAMs involves the immobilization of two alkane thiols, one bearing the ligand of interest, onto the gold-coated tip. A low ratio of ligands *vs*. alkane thiols has to be used (generally 1 : 99) in order to "dilute" the ligand within the matrix formed by the alkane thiols (Fig. 25).

In this way, the density of ligands at the surface of the tip is sufficiently low to permit the detection of single interactions with the complementary receptor and to prevent unwanted steric hindrance in the recognition process.

By following this strategy, Vansco *et al*. have studied by AFM the rupture forces of individual host–guest complexes between β-cyclodextrin (β-CD) heptathioether (Fig. 26a) monolayers on a gold surface and a limited number of guest molecules confined on the surface of gold-coated AFM tips prepared by the formation of mixed SAMs (Fig. 26b).[77,78] This study was based on the ability of β-CD to form inclusion complexes with a variety of neutral and charged organic molecules, such as ferrocene, mainly *via* hydrophobic interactions.

A gold-coated tip was modified with mixed SAMs of 2-mercaptoethanol containing 0.2 to 1% of thiol-modified ferrocene (guests) (Fig. 26b). Mixed SAMs were prepared from 1 mM (total thiol concentration) solutions in ethanol over 16 h at room temperature.

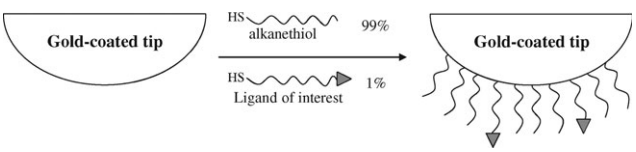

Fig. 25 Schematic illustration of mixed SAM preparation.

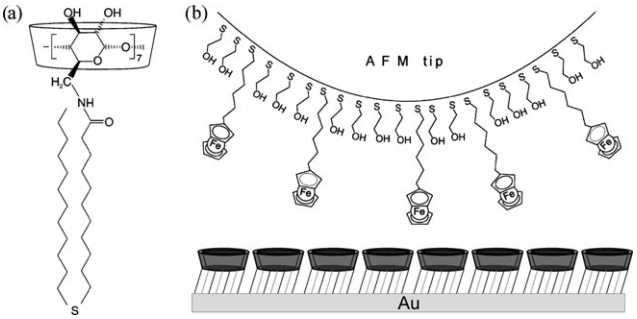

Fig. 26 SMRFM experiment for the measurement of rupture forces of individual host–guest complexes between β-cyclodextrin and ferrocene.[77,78] (a) β-CD derivative β-CD-$(OH)_{14}$. (b) General scheme of the SMRFM experiment.

Force–distance experiments were performed by probing the β-CD surface with the ferrocene-modified tip. A representative force–displacement curve is presented in Fig. 27, showing single, as well as characteristic multiple, pull-off events. The occurrence of multiple individual pull-off events during retraction of the tip from the sample was attributed to the rupturing of host–guest complexes in the retracting contact area between the probe and surface.

Furthermore, Vansco *et al*. have estimated that the number of ferrocene-terminated molecules (14–28) at the contact area of the substrate SAM and the AFM tip,[78] by using Johnson–Kendall–Roberts' theory.[79] They made a correlation with the number of individual pull-offs observed in the AFM experiments (10–20). They attributed the occurrence of multiple pull-offs to the slightly different distances between the ferrocenes and the β-CD surface, due, for example, to the curvature of the AFM tip and the granular nature of the gold on the tip.

Similarly, Schmitt *et al*. have modified an AFM tip with mixed SAMs of alkane thiols (triethylene glycol alkyl thiol: EO_3-thiol) and an *N*-nitrilo-triacetic acid thiol derivative (NTA triethylene glycol alkyl thiol: NTA-thiol) in order to study molecular forces of the NTA/His-tag complex (Fig. 28).[80]

The tetradentate ligand NTA forms a hexagonal complex with divalent metal ions such as Ni^{2+}, occupying four of the six binding sites. The remaining two binding sites are accessible to electron donor groups, such as histidine. Force measurements of

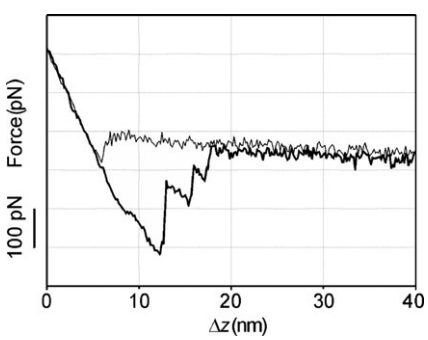

Fig. 27 Representative force–distance curve for host–guest complexes between a β-CD derivative and ferrocene. The tip approach curve (bright line) and the retracting curve (dark line) are shown.[78]

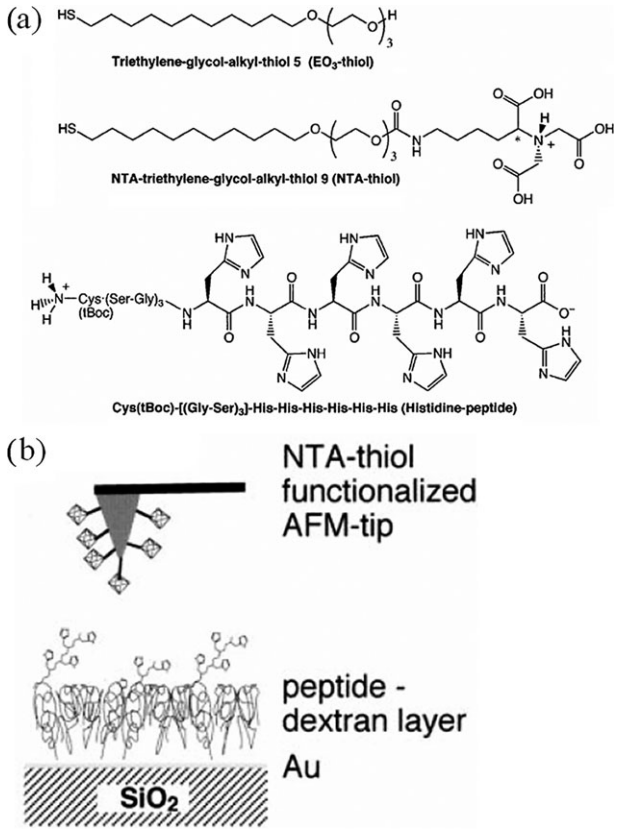

Fig. 28 A study of the molecular forces of the NTA/His-tag complex by SMRFM.[80] (a) The molecules used to functionalize the AFM tip (EO_3-thiol and NTA-thiol) and sample surface (histidine peptide). (b) General scheme of the SMRFM experiment between the NTA-functionalized tip and the histidine-functionalized surface.

the binding, in presence of Ni^{2+} ions, between NTA ligand, anchored to an AFM tip, and a polyhistidine peptide, supported on a surface, were investigated in their study.

Mixed SAMs were prepared by incubating a gold-coated tip in 1 mM solutions of EO_3-thiol/NTA-thiol (9 : 1, mol%/mol%) in ethanol for 12–20 h. The histidine-rich peptide was covalently attached to carboxymethyl-dextran-coated gold surfaces. According to the protocol used, the authors estimated that no more than 40% of the potential binding sites on the polymer were derivatized with the ligand.

By both diluting the NTA ligand on the tip (by using mixed SAMs) and the histidine peptide on the surface, Schmitt *et al.*[80] rarely observed more than one event (<5%), and in most of the force scans, only one bond rupture was detectable (75%). No events were measured in about 20% of scans.

Berquand *et al.* recently used the NTA/Ni^{2+}/His-tag system described above to anchor an antibody in order to explore the binding force with its complementary antigen (lysozyme), as illustrated in Fig. 29.[81]

The tip was functionalized as described above with mixed SAMs from EG-alkane thiols and NTA-alkane thiols in a 95 : 5 ratio. Fv antibodies were anchored to the NTA functionality *via* the formation of the NTA-His system. Lysozyme was covalently immobilized on the mixed SAMs of carboxyl- and hydroxyl-terminated alkane thiols (ratio 20 : 80) on the gold surface.

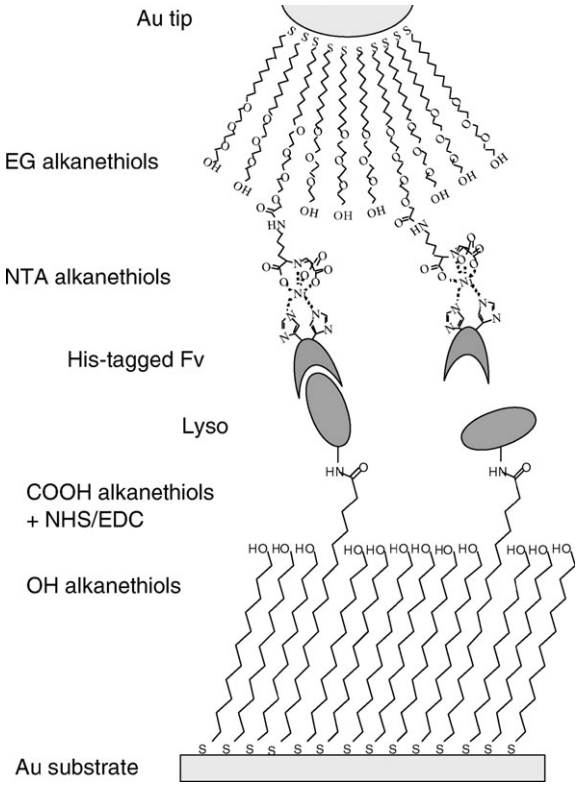

Fig. 29 Schematic representation of a SMRFM experiment for the study of the binding force of an antibody and its antigen (lysozyme) using the NTA/His anchoring system.[81]

Unfortunately, force–distance experiments showed that only 26% of unbinding events were recorded, and that both single and multiple unbinding forces were displayed. This relatively low unbinding force frequency was attributed by the authors to the low density of biomolecules attached to the tip and substrate, as well as to the random orientation of the Lyso molecules.

To summarize, the use of mixed SAMs to functionalize AFM tips, as well as the surface substrate as described in the two last examples,[80,81] constitutes an efficient way to decrease the density of ligands and hence permit the detection of single molecule interactions between hosts and guests. However, the difficulty lies in controlling the composition of the mixed SAMs, and therefore on the reproducibility of experiments. Nevertheless, the ease of preparing modified tips and surfaces makes this strategy very appealing for developing useful systems to study important recognition phenomena at the single molecule level.

In addition to mixed-SAMs, the setting-up of small tip–substrate contacts by using sharper tips would allow single bond detection.

3.3 Towards single molecule functionalization

A few other ways to obtain single molecule detection have been described in the literature.

3.3.1 Selective electrooxidation of OEG-coated tips. Working towards single molecule detection, Cai *et al.* improved the system described in section 3.2.1.2[66] by tethering tips with a

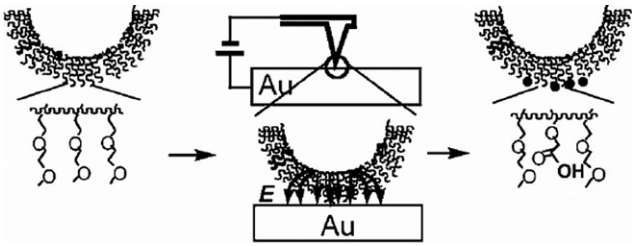

Fig. 30 Illustration of the selective electrooxidation of OEG-coated tips to yield tips with very few carboxylic acid groups at the apex.[82]

defined number of probe molecules at the tip apex.[82] Indeed, they have shown that OEG-coated tips, whose preparation is illustrated in Fig. 20, can be selectively modified at the tip apex by electrooxidation to generate very few terminal carboxylic acid groups (Fig. 30).

The electrochemical reaction was undertaken by connecting the coated tip and a flat Au(111) electrode to a voltage pulse generator. The tip was then engaged with the gold surface in contact mode, and a brief voltage pulse applied to the gold electrode while the tip was grounded. In this way, only OEG end groups in contact with the gold electrode at the tip apex were oxidized to generate COOH groups.

These OEG-coated tips were derivatized to attach biomolecules for the measurement of specific interactions with target molecules. In this strategy, an amino-terminated biotinylated compound was coupled to the tip by its reaction with one carboxylic acid group to generate a mono-biotinylated tip (Fig. 31). This tip was further used to study single molecule adhesion force measurements between the tip-supported biotin and an avidin-coated surface.

This approach is one of the most versatile, allowing the preparation of well-defined AFM tips for probing single target molecules.

3.3.2 Low surface density functionalization of a silicon tip with ethanolamine. This approach is based on the functionalization of a tip at very low concentrations, so allowing the fixation of very few probes. In this way, alkane monolayers are formed on the silicon tip surface by an ''etherification'' reaction, forming Si–O–C bonds. The most commonly found example in the literature is the reaction of surface silanol groups with ethanolamine (Fig. 32). Amino groups are thus generated at a low surface density on the tip, corresponding to few sites per tip apex, as necessary for single molecule experiments.[83]

This tip functionalization method with ethanolamine has been extensively used by Hinterdorfer *et al.* to anchor various biological ligands *via* a polyethylene glycol tethering group in

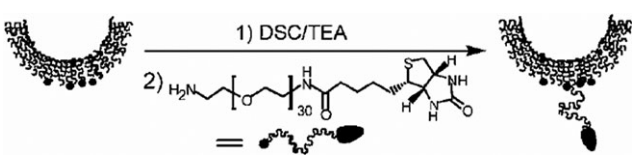

Fig. 31 Preparation of a mono-biotinylated tip from a carboxylic acid-modified tip.[82]

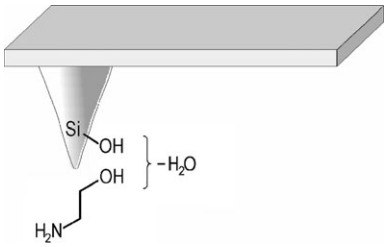

Fig. 32 Silicon surface etherification with ethanolamine.[83]

single molecule recognition force investigations.[83] These studies will be discussed in more detail in section 4.1.

4. Transducers

Besides the AFM tip functionalizations described above, another approach investigated has been to incorporate spacer molecules between the tip and ligands of interest. These anchor arms have been proposed to promote specific receptor–ligand recognition and to transduce the signal from the recognition event to the tip. In this section, we review efforts in this area with work on polyethylene glycol (PEG) and carbon nanotubes (CNTs) as possible molecular transducers.

4.1 Polyethylene glycol

The use of a flexible spacer molecule, such as PEG, to tether ligands to AFM tips was first reported by Hinterdorfer *et al.* for the study of antibody–antigen recognition.[84] This methodology was developed to overcome previous failures, attributed to a lack of molecular mobility and unspecific tip–probe adhesion forces obscuring specific interactions.[85]

4.1.1 Properties and advantages of PEG linkers. The insertion of a PEG spacer between the probe molecule and the apex of the measuring tip has been described as affording significant technical improvements:[86,87]

- The PEG spacer allows the probe molecule to freely reorient for unconstrained receptor–ligand recognition.
- The probe molecule can scan a large surface for target molecules during a tip–substrate encounter.
- The probe molecule can escape the danger of being crushed between the tip and substrate during hard contact.
- The soft and non-linear elasticity of the PEG tether allows unspecific and receptor-specific binding of the tip to be clearly distinguished.

4.1.2 Synthesis of PEG derivatives. One example of an efficient PEG tether design is illustrated in Fig. 33.[87] The linker is a heterobifunctional PEG derivative of 18 units, corresponding to an 8 nm extended length, with a *N*-hydroxysuccinimide (NHS) ester function to allow the fixation onto an amino-modified tip and a thiol-reactive end group (2-(pyridyldithio)propionyl; PDP) to couple the thiol-containing probe molecule.

For the synthesis of the linker, a diamine derivative of PEG served as the starting material (Fig. 34). The sulfide function was inserted by the protection of one amine group with *N*-succinimidyl-3-(*S*-acetylthio)propionate (SPDP); the resulting dissymmetric product was easily isolated from the statistical

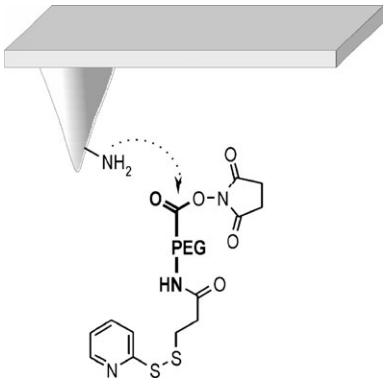

Fig. 33 Design of the heterobifunctional PEG derivative that allows the fixation onto an amino-modified tip *via* its NHS ester function and the coupling of thiol-containing probe molecule *via* its thiol-reactive end group.[87]

mixture of unreacted diamine and symmetric product. After reaction of the remaining amine with glutaric anhydride, the resulting carboxylic acid function was activated with NHS to afford the heterobifunctionnal PEG derivative.[88]

4.1.3 Linkage onto NH_2 tips. AFM tips were first functionalized with amines by bonding ethanolamine hydrochloride to the silicon tip surface, as described previously (*cf.* section 3.3.2). The PEG linker can be then covalently coupled to the amines on the tip surface *via* its NHS ester end. This kind of functionalization enables the anchoring of a ligand of interest as the last step by coupling of its thiol function to the thiol-reactive end of the PEG derivative. Therefore, this strategy is applicable to a wide range of biologically-relevant probes.

The surface density of ligands on tips was chosen to be sufficiently low so that, on average, only one of the flexibly-linked ligands was expected to be bound to the tip end that was accessible to its complementary receptor on the probe surface.

4.1.4 Applications in SMRFM experiments. Hinterdorfer *et al.* have used a PEG cross-linker to tether various biological ligands to AFM tips in order to detect receptor–ligand interactions at the single molecule level. Amongst the studies reported, we will focus on three systems illustrated in Fig. 35: the biotin–avidin system (Fig. 35a), an antibody–antigen recognition system (Fig. 35b) and the NTA–histidine complex (Fig. 35c).

Tip functionalization was performed in all three cases as described above.[87] Measurements of the interaction forces of biotin–avidin pairs were undertaken by probing an avidin-coated mica surface with a biotin-functionalized AFM tip, and recording several consecutive force–distance cycles. The results are shown in Fig. 36. It may be noticed that only single molecular unbinding forces were measured, further validating the process of tip functionalization. Moreover, non-specific adhesion events between the tip and mica were characterized by a non-elastic and linear trace upon retraction (Fig. 36b), whereas force–distance cycles in specific recognition events showed an elastic and linear retrace (Fig. 36a). This pattern is characteristic of the well-known non-linear stretching of PEG and shows that this linker acts as a rubber band between the tip and the surface. In this way, the stretching of the polymer improves the transduction of the molecular recognition signal to the AFM tip into a mechanically measurable force (cantilever deflection).

The efficiency of this system was estimated by recording binding events between biotin and avidin. In 476 consecutive force–distance measurements performed with the same tip, 136 similar unbinding events were observed, corresponding to a binding probability of 29%.

In comparison, by using a longer PEG chain (35 nm) to tether biotin to the tip, Joselevich *et al.* estimated a binding probability of 20%.[90] Consequently, even if the PEG cross-linker promotes specific binding of the ligand to receptor sites on the surface by freely reorienting probe molecules, tethers that are too long and flexible seem to decrease binding probability.

Advantages of the flexibility of PEG cross-linkers were outlined during a study of antibody–antigen recognition (Fig. 35b).[84] Anti-human serum albumin (HSA) antibody was first pre-derivatized by activating its lysine residues with the short linker *N*-succinimidyl-3(*S*-acethylthio)propionate (SATP). The resulting thiol function was then coupled to the PEG cross-linker previously anchored to the tip. By probing the HSA antigen-coated surface with this antibody-functionalized tip, half of force–distance cycles showed one or two unbinding events between these two partners. However, the potential of the sensor for localizing individual antigenic sites was analyzed by preparing a diluted HSA surface (about 15 times lower density than was used initially). In this case, only single recognition events were recorded, indicating that only one HSA molecule was available for antibody binding. It has been estimated that the 8 nm-long flexible spacer allowed the antibody to bind to a HSA molecule within a distance of 6 nm around the momentary position of the scanning tip, demonstrating that this cross-linker is sufficiently flexible and long for the effective and fast recognition of antigens, and sufficiently short for their accurate localization.

Besides this covalent coupling of probe molecules to AFM tips, Hinterdorfer *et al.* developed an attractive alternative

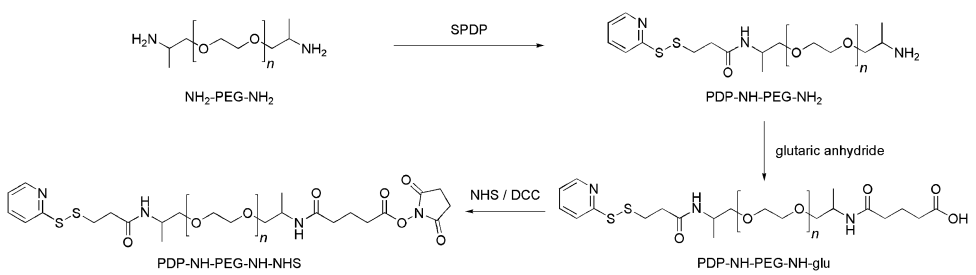

Fig. 34 Synthesis of a heterobifunctional PEG derivative.[88]

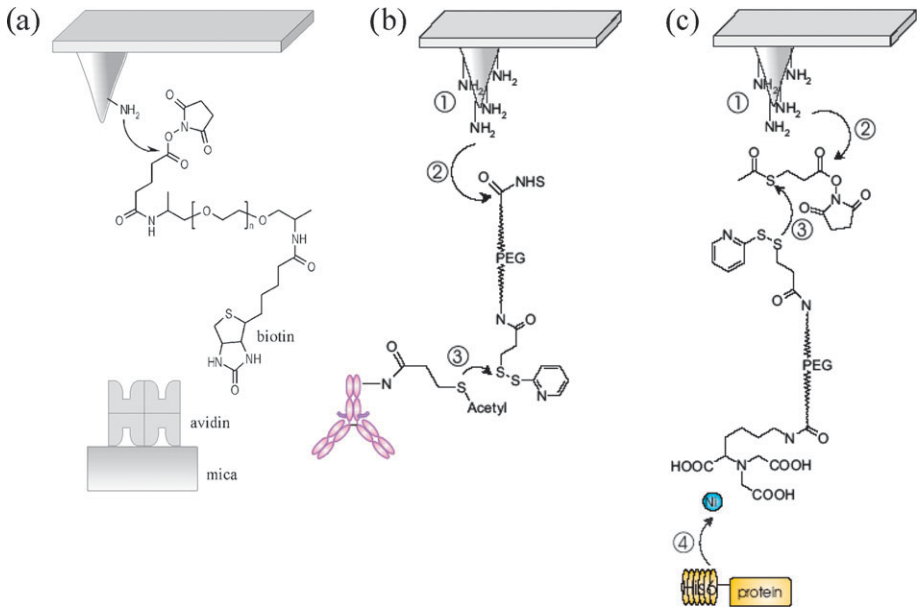

Fig. 35 Schematic representations of tip functionalization for the recognition study of (a) a biotin–avidin system, (b) an antibody–antigen system and (c) a NTA–His complex.[87,89]

provided by the widely used nitrilo-triacetate (NTA)–Ni^{2+}–His_6 system (Fig. 35c).[91] The binding of this system was shown to be significantly larger than that between most ligand–receptor pairs, allowing this system to be used to anchor probe molecules. Moreover, this system opens the way to a reversible linkage process.

Tip functionalization proceeds as follows: the NH_2-functionalized tip was derivatized with mercaptopropionyl groups, to which PDP–PEG–NTA was coupled *via* a disulfide linkage. In the presence of Ni^{2+}, His_6-tagged protein can be tightly bound to the NTA–Ni^{2+} function, as already described in the third part of this review (Fig. 29).

This system was recently used to probe human rhinovirus serotype 2 (HRV2) by coupling its complementary His_6-tagged ligand MBP-VLDLR1-3 (Fig. 37).[87]

Finally, depending on the situation, one or other method can be used. Non-covalent coupling would be the method of choice if the probe molecule is available as a His_6-tagged protein. In contrast, covalent coupling is more appropriate for short term studies with untagged proteins or other probe molecules.

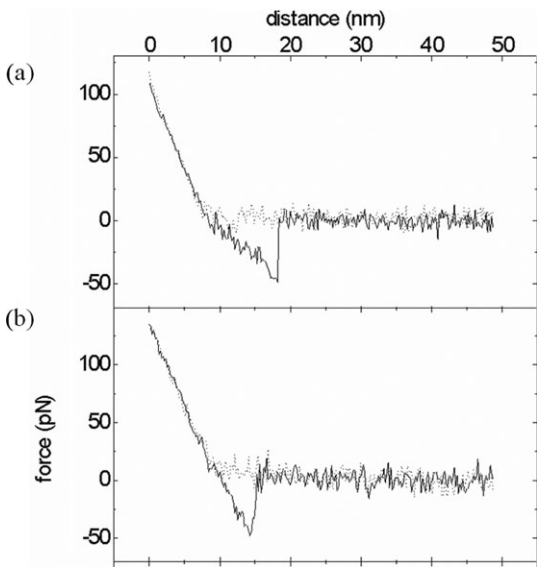

Fig. 36 Force spectroscopy of single avidin–biotin interactions using a PEG transduction system.[87] (a) Force–distance cycle (tip approach in dotted line and retracting in solid line) showing specific avidin–biotin binding. (b) Force–distance cycle showing unspecific binding to the mica substrate.

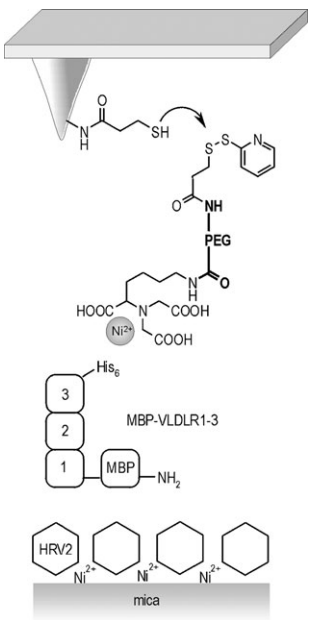

Fig. 37 Flexible tethering of a His_6-tagged probe molecule (MBP-VLDLR1-3) to an AFM tip for the detection of human rhinovirus serotype 2 (HRV2).[87]

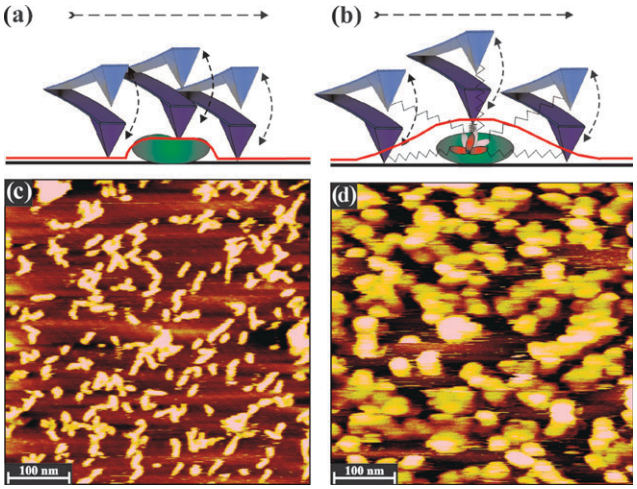

Fig. 38 Topography (a,c) and molecular recognition (b,d) imaging processes of an antigen-coated surface probed by an antibody-tethered tip.[92]

To summarize, use of a PEG cross-linker for tethering probe molecules to tips promotes specific unconstrained receptor–ligand recognition by providing translational and rotational degrees of freedom that are necessary for the ligand to reach its complementary receptor on the sample substrate. In this way, the ligand can freely orient and diffuse within a certain volume, as determined by the length of the tether. Moreover, the PEG-linker polymer can transduce the configurational constraint imposed by receptor–ligand molecular recognition into a measurable force. This force is defined by the entropic elasticity of the polymer and is characterized by a strong non-linearity. These properties give rise to oscillations of the probe cantilever upon molecular recognition.[90]

Hinterdorfer *et al.* have exploited these properties of transduction to investigate molecular recognition imaging of systems tethered to a tip *via* PEG transducers.[89]

Studies by dynamic force microscopy of an antigen-coated surface probed by an antibody-tethered tip are shown in Fig. 38.[92]

As presented in Fig. 38b, the antibody on the tip binds to the antigen before the tip is above the antigenic site because of the flexible tethering provided by the PEG spacer. At this point, the attractive force of the cross-linker, acting as a nanospring, is smaller than that when the tip is directly above the antigen. This induces a smaller decrease in tip oscillation amplitude. Thus, variations in the z-oscillation of the cantilever are representative of the antibody–antigen recognition forces, transduced by the elastic PEG spacer, allowing molecular recognition imaging (Fig. 38d) that fits to the topography imaging obtained with a bare tip (Fig. 38a and c).

Advances have also been made in obtaining simultaneous topography and molecular recognition imaging. The principle of this technique is based on the electronic split of the recorded cantilever oscillation during molecular recognition measurements into lower and upper parts, resulting in simultaneous topography and recognition images (Fig. 39).[93]

Fig. 40 shows an example of the cantilever oscillation while scanning along a surface. Both the maxima and minima of the oscillation periods are influenced by interactions between the tip and surface. Variations in the minima are directly related to topography data: the scanning of a molecule on the surface induces a reduction of the tip oscillation because of the height of the sample. On the contrary, variations in the maxima provide data for image recognition: binding of the probe tip to the substrate by receptor–ligand recognition restricts tip motion and reduces tip oscillations.

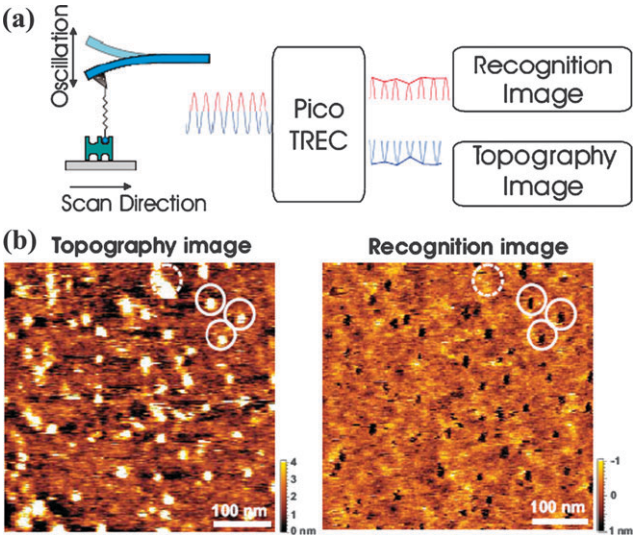

Fig. 39 Topography recognition imaging (TREC).[93] (a) Principle: The cantilever oscillation is split into lower and upper parts, resulting in the simultaneous acquisition of topography and recognition images. (b) The topography (left) and recognition (right) images for a biotin–avidin system show good correlation.

This imaging technique was applied successfully to perform simultaneous topography and recognition imaging of a biotin–avidin system,[93] as well as an antibody–antigen pair.[94,95]

4.2 Carbon nanotubes (CNTs)

The fabrication and the characterization of a new generation of tips based on carbon nanotubes were reported at the end of the 1990s by Lieber *et al.*[96,97] Functionalization of tips with CNTs was first investigated to improve the properties of commercial silicon tips for imaging, and was further used in chemical force microscopy experiments, as well as single molecule force spectroscopy.

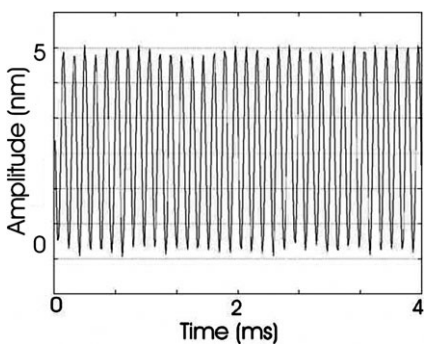

Fig. 40 An example of the deflection signal of a magnetically-oscillated cantilever during scanning along the surface.[89]

4.2.1 Properties and advantages of CNTs. Carbon nanotubes represent ideal AFM tip materials due to their diameter (as small as 1 nm), which confers upon them a high aspect ratio for imaging deep and narrow features, and, for single-walled nanotubes (SWNTs), great potential to have resolutions under 0.5 nm. For instance, SWNT tips have radii of curvature of 2–4 nm, representing an important improvement over commercial silicon tips (10–50 nm).

Moreover, CNTs present considerable mechanical flexibility, and the ability to elastically buckle.[98] These findings are very important for the use of CNTs in tip functionalization because of the necessary robustness of such materials. Indeed, these features would prevent the tip from being damaged during imaging or other AFM experiments, and the capacity to buckle elastically would improve the transduction of the molecular recognition signal to the tip.

Finally, CNTs seem to have very small non-specific adhesion on mica or other sample surfaces, and can be functionalized with chemical and biological probes at the tube ends.

4.2.2 Functionalization of silicon tips with CNTs. The first CNT tips were fabricated by the direct mechanical assembly of multi-walled (MWNTs) or single-walled carbon nanotubes (SWNTs) on silicon tips. Bonding between the nanotubes and the tip was achieved using a soft acrylic adhesive, and controlled by optical or electron microscopy.[98] Mechanical attachment was further improved by transferring a single aligned nanotube onto a silicon tip under the view of a scanning electron microscope, followed by the attachment of the nanotube by deposition of amorphous carbon.[99] Using these methods, nanotube bundles rather than individual nanotubes were attached to tips, with a relatively long period of time being required to make one tip. Moreover, it was not possible to reproducibly prepare individual SWNT tips.

To overcome these limitations, Lieber *et al*. developed a technique of growing individual CNT probe tips directly by chemical vapor deposition (CVD).[100,101]

This method, also called pore growth, is shown schematically in Fig. 41.

This nanotube tip preparation followed a three step procedure. A conventional silicon tip was first flattened at its apex by contact AFM imaging and by anodizing it in hydrogen fluoride to create nanopores of 50–100 nm along the tip axis. Iron oxide nanoparticles, used as the catalyst for nanotube growth, were then electrodeposited into the pores. Growing of the nanotubes was finally performed by CVD, according to the process described in Fig. 42. The oriented pore structure thus controlled the direction of growth.

Metal catalyst particles are heated in the presence of a hydrocarbon gas (ethylene) or carbon monoxide. The reactant molecules dissociate onto the surface of the metal catalyst particle and carbon is adsorbed onto it. When this carbon precipitates, it nucleates to form a nanotube of similar diameter to the catalyst particle.

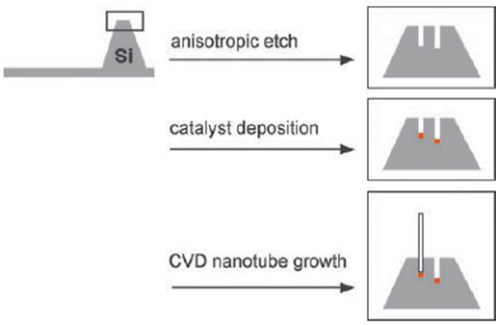

Fig. 41 The pore growth technique for CVD nanotube-modified tip production.[101]

Experimental improvements have been made to promote the formation of SWNTs *vs*. MWNTs. However, limitations still remain in obtaining individual SWNTs. Lieber *et al*. supposed that better control of the catalyst density should improve the formation of individual *vs*. bundle SWNT tips.[101]

An attractive alternative to the pore growth approach is the surface growth method, which exploits the CVD technique for nanotube tip preparation, but avoids the need for creating nanopores. In this approach, the catalyst is first deposited onto the pyramidal tip, and then CVD is used to grow the SWNT probe (Fig. 43).[102]

This technique is based on the property that nanotubes have of preferring to grow along a surface due to an attractive nanotube–surface interaction. Therefore, nanotubes will generally bend in order to stay in contact rather than grow out from a surface when they encounter an edge. In this way, nanotubes will grow along the surface until they reach the pyramidal edges, where they will be directed towards the tip apex along these edges. At the tip apex, because nanotube–surface interactions are smaller, nanotubes will protrude straight from the apex (*vs*. bending) to create an almost ideal tip (Fig. 44).

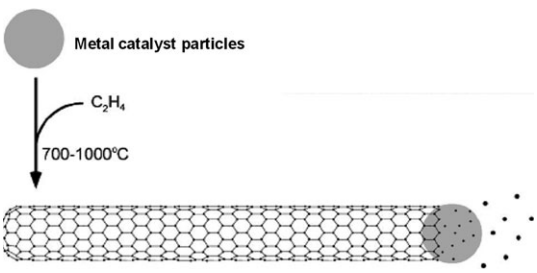

Fig. 42 Nanotube production by CVD.[97]

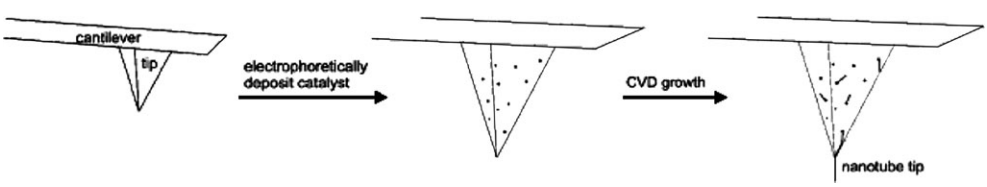

Fig. 43 Overview of the surface growth technique, which allows the preparation of a SWNT at the tip apex.[102]

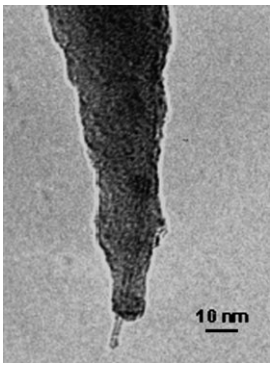

Fig. 44 TEM image of an individual SWNT tip produced by surface growth.[96]

It has been shown that the use of Fe–Mo and colloidal iron oxide catalysts at a low density promotes the formation of individual SWNTs. It was also estimated that nanotubes typically protrude from the edges of the pyramid with a density of approximately one per micron, and that at least 90% of pyramids had a nanotube protruding directly from the apex.

It should also be noted that these grown nanotubes are generally too long for AFM experiments, but that they can easily be shortened using a straightforward electrical etching method.

In summary, by using this surface growth technique, well-defined individual SWNT-modified tips can be reproducibly formed.

4.2.3 Chemical condensation of CNTs on NH_2 tips. Hiura *et al*. have shown that open-end nanotube tips can be formed by shortening the tubes in an oxidizing environment, forming carboxyl groups at these open ends.[103]

Yang *et al*. used this interesting property to develop a wet chemical approach based on the condensation reactions between amino end groups of SAM surfaces and carboxyl groups on CNTs to attach SWNTs onto AFM tips (Fig. 45).[104]

Gold-coated tips were first incubated with amino-undecanethiol to form a densely-packed amino-terminated SAM at the tip surface. After activation with dicyclohexylcarbodiimide (DCC), COOH-terminated CNTs were attached to the amine function. It was estimated that the density of nanotubes on AFM tips was relatively low, and that it was possible that only

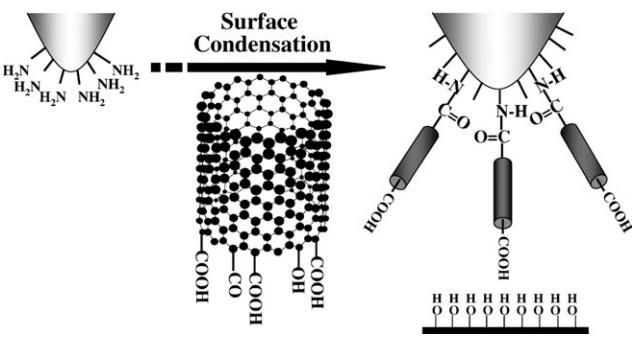

Fig. 45 Preparation of SWNTs modified AFM tips by chemical condensation.[104]

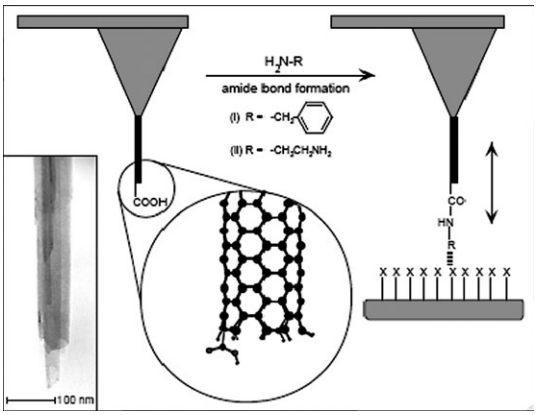

Fig. 46 Preparation of functionalized CNT-modified tips for CFM experiments.[108]

a single nanotube, or one bundle of nanotubes, could be attached to the end of AFM tips.

4.2.4 Utilization of CNT-modified tips for topographical imaging. Because of their intrinsic properties, tips functionalized with SWNTs have been used for topographical imaging. Firstly, they have small diameters (about 1 nm for SWNTs) that offer the potential for very significant improvements in lateral resolution. Secondly, because nanotubes can elastically buckle, they can prevent damage to and deformation of biological samples. Several examples of the topographical imaging of biological samples have been reported by Lieber *et al*., including immunoglobulin G[96,97] and DNA.[105–107]

4.2.5 Utilization of CNT-modified tips for functional imaging and force measurements. Lieber *et al*. have shown that CNTs can be functionalized with specific biological probes for functional imaging and force measurements.[96,97,108]

Covalent modifications of nanotube modified tips have been investigated by coupling various amines to open-ended nanotube carboxyl groups[103] *via* carbodiimide chemistry (Fig. 46).

The first example was investigated for chemically-sensitive imaging using patterned SAM substrates in CFM experiments.[109]

Benzylamine was used to create a hydrophobic tip, which was used to discriminate between $-CH_3$ and –COOH functional groups on a surface (Fig. 47).

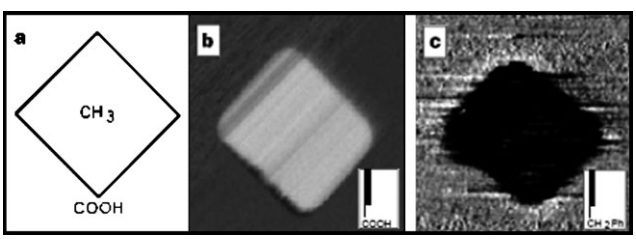

Fig. 47 Chemically-sensitive imaging with functionalized nanotube tips.[108] (a) Representation of CH_3- and COOH-terminated SAM regions of the sample substrate. (b) Image of the friction force recorded with an unmodified nanotube tip. The darker regions correspond to a high friction force. (c) Image of the friction force recorded with a benzylamine-functionalized nanotube tip.

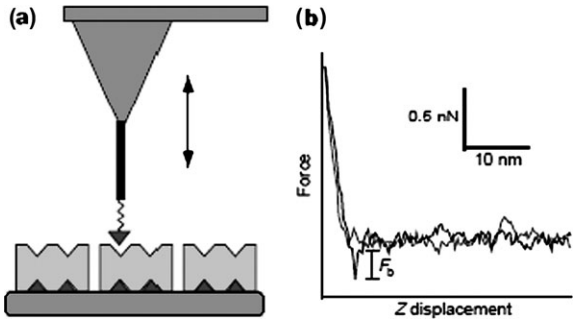

Fig. 48 Biotin-derivatized nanotube tips as biological probes for SMRFM. (a) Schematic drawing illustrating force measurement experiment between a biotin-derivatized nanotube tip and a streptavidin surface. (b) Force–distance cycle showing streptavidin–biotin binding (the grey line represents tip approach and the black one tip retraction).[108]

Similarly, in order to investigate force–displacement measurements with a streptavidin-coated surface, biotin was conveniently linked to nanotube-modified tips (Fig. 48). The results reported for this study on two modified tips showed that, for the first tip only, unbinding of a single biotin–streptavidin ligand receptor was recorded in 36% of measurements (no detectable binding was recorded in the remaining 64% of events). For the second tip, both single and double unbinding forces were measured. In this case, 30% of measurements were attributed to single binding events, whereas double binding events occurred 15% of the time.

To sum up, it has been shown that a single active ligand can be specifically anchored at the end of a nanotube tip using well-defined covalent chemistry. This property has allowed the study of ligand–receptor binding at the single molecule level and improved the resolution of investigative topographical imaging. Moreover, the capacity of nanotubes to buckle elastically allows enhanced transduction of the molecular recognition signal into a measurable force. Finally, it may be noted that the system based on the nanotube-functionalization of tips is more efficient than that using PEG. This may be explained by the fact that, compared to PEG spacers, CNT spacers provide better orientational control of the probe molecules by reducing their degrees of freedom.

Conclusions and outlook

In this review, the main chemical strategies to functionalize AFM tips have been described. Among the various applications of AFM, focus has been particularly directed on the study of single molecule experiments, and consequently on the functionalization of AFM tips with one or few molecules. Few strategies, such as the electrooxidation of OEG-coated tips (*cf.* section 3.3.1) and the direct growing of CNT at the apex of tips (*cf.* section 4.2), seem to allow single molecular detection. In the other cases, it seems to be difficult to control the density of the target molecule on tips (especially at the apex) and to measure single bond forces. The set-up of small tip–substrate contacts, using sharper tips and a low density of molecules on the tip, can improve single contact detection, but generally, further analysis is required to discriminate single bond forces from among multiple measured forces.

To conclude, the selective modification of AFM tips hold great promise towards affording unique tools to investigate important biological recognition phenomena at the single molecule level. While the reported approaches demonstrate tremendous originality and are based on impressive scientific breakthroughs, there is still a need for general, simple and sturdy synthetic procedures that will provide easily- and reproducibly-modified tips of predetermined spatial distribution. This will come true by multi-disciplinary collaborative research efforts between scientists with diverse but complementary expertise. With the tremendous success achieved so far, the future of single molecule studies based on AFM has never been so bright.

Acknowledgements

The authors thank the NSERC of Canada, NanoQuebec, the FQRNT of Quebec and the Laval University of Quebec, Canada for their financial support of this work.

Notes and references

1 G. Binnig, C. F. Quate and Ch. Gerber, *Phys. Rev. Lett.*, 1986, **56**(9), 930–933.
2 Z. Shao, J. Mou, D. M. Czajkowsky, J. Yang and J.-Y. Yuan, *Adv. Phys.*, 1996, **45**(1), 1–86.
3 S. Allen, S. M. Rigby-Singleton, H. Harris, M. C. Davies and P. O'Shea, *Biochem. Soc. Trans.*, 2003, **31**(5), 1052–1057.
4 W. Han, S. M. Lindsay and T. Jing, *Appl. Phys. Lett.*, 1996, **69**(26), 4111–4113.
5 H. Schindler, D. Badt, P. Hinterdorfer, F. Kienberger, A. Raab, S. Wielert-Badt and V. P. Pastushenko, *Ultramicroscopy*, 2000, **82**, 227–235.
6 G. Ge, D. Han, D. Lin, W. Chu, Y. Sun, L. Jiang, W. Ma and C. Wang, *Ultramicroscopy*, 2007, **107**, 299–307.
7 A. Rosa-Zeiser, E. Weilandt, S. Hild and O. Marti, *Meas. Sci. Technol.*, 1997, **8**, 1333–1338.
8 T. Miyatani, M. Horii, A. Rosa, M. Fujihira and O. Marti, *Appl. Phys. Lett.*, 1997, **71**(18), 2632–2634.
9 A. Engel, C.-A. Schoenenberger and D. J. Müller, *Curr. Opin. Struct. Biol.*, 1997, **7**, 279–284.
10 C. Bustamante, D. A. Erie and D. Keller, *Curr. Opin. Struct. Biol.*, 1994, **4**, 750–760.
11 H. G. Hansma and J. H. Hoh, *Annu. Rev. Biophys. Biomol. Struct.*, 1994, **23**, 115–139.
12 J. Fritz, D. Anselmetti, J. Jarchow and X. Fernàndez-Busquets, *J. Struct. Biol.*, 1997, **119**, 165–167.
13 S. Kasas, N. H. Thomson, B. L. Smith, P. K. Hansma, J. Miklossy and H. G. Hansma, *Int. J. Imaging Syst. Technol.*, 1997, **8**, 151–161.
14 A. V. Bolshakova, O. I. Kiselyova and I. V. Yaminsky, *Biotechnol. Prog.*, 2004, **20**, 1615–1622.
15 K. J. Kwak, H. Kudo and M. Fujihira, *Ultramicroscopy*, 2003, **97**, 249–255.
16 C. Bustamante, C. Rivetti and D. J. Keller, *Curr. Opin. Struct. Biol.*, 1997, **7**, 709–716.
17 A. Engel and D. J. Müller, *Nat. Struct. Biol.*, 2000, **7**(9), 715–718.
18 A. Noy, D. V. Vezenov and C. M. Lieber, *Annu. Rev. Mater. Sci.*, 1997, **27**, 381–421.
19 E. W. van der Vegte and G. Hadziioannou, *Langmuir*, 1997, **13**, 4357–4368.
20 A. Noy, C. D. Frisbie, L. F. Rozsnyai, M. S. Wrighton and C. M. Lieber, *J. Am. Chem. Soc.*, 1995, **117**, 7943–7951.
21 A. Noy, C. H. Sanders, D. V. Vezenov, S. S. Wong and C. M. Lieber, *Langmuir*, 1998, **14**, 1508–1511.
22 J. Zlatanova, S. M. Lindsay and S. H. Leuba, *Prog. Biophys. Mol. Biol.*, 2000, **74**, 37–61.

23 A. Janshoff, M. Neitzert, Y. Oberdörfer and H. Fuchs, *Angew. Chem., Int. Ed.*, 2000, **39**, 3212–3237.
24 T. Hugel and M. Seitz, *Macromol. Rapid Commun.*, 2001, **22**, 989–1016.
25 A. Ptak, S. Takeda, C. Nakamura, J. Miyake, M. Kageshima, S. P. Jarvis and H. Tokumoto, *J. Appl. Phys.*, 2001, **90**(6), 3095–3099.
26 M. Kageshima, M. A. Lantz, S. P. Jarvis, H. Tokumoto, S. Takeda, A. Ptak, C. Nakamura and J. Miyake, *Chem. Phys. Lett.*, 2001, **343**, 77–82.
27 S. Tadeka, A. Park, M. Kageshima, H. Tokumoto, C. Nakamura and J. Miyake, *Surf. Sci.*, 2003, **532–535**, 244–248.
28 M. Ludwig, M. Rief, L. Schmidt, H. Li, F. Oesterhelt, M. Gautel and H. E. Gaub, *Appl. Phys. A: Solid Surf.*, 1999, **68**, 173–176.
29 S. Zou, H. Schönherr and G. J. Vansco, *Angew. Chem., Int. Ed.*, 2005, **44**, 956–959.
30 C. Ortiz and G. Hadziioannou, *Macromolecules*, 1999, **32**, 780–787.
31 A. Noy, D. V. Vezenov, J. F. Kayyem, T. J. Meade and C. M. Lieber, *Chem. Biol.*, 1997, **4**, 519–527.
32 S. Allen, J. Davies, A. C. Dawkes, M. C. Davies, J. C. Edwards, M. C. Parker, C. J. Roberts, J. Sefton, S. J. B. Tendler and P. M. Williams, *FEBS Lett.*, 1996, **390**, 161–164.
33 www.nanosensors.com.
34 www.nanotechnology.net.
35 T. R. Albrecht, S. Akamine, T. E. Carver and C. F. Quate, *J. Vac. Sci. Technol., A*, 1990, **8**(4), 3386–3396.
36 D. J. Keller and C. Chih-Chung, *Surf. Sci.*, 1992, **268**, 333–339.
37 K. I. Schiffmann, *Nanotechnology*, 1993, **4**, 163–169.
38 H. Ximen and P. E. Russell, *Ultramicroscopy*, 1992, **42–44**, 1526–1532.
39 H. Takano, J. R. Kenseth, S.-S. Wong, J. C. O'Brien and M. D. Porter, *Chem. Rev.*, 1999, **99**, 2845–2890.
40 H. F. Knapp and A. Stemmer, *Surf. Interface Anal.*, 1999, **27**, 324–331.
41 C. Mihalcea, W. Scholz, S. Werner, S. Münster, E. Oesterschulze and R. Kassing, *Appl. Phys. Lett.*, 1996, **68**(25), 3531–3533.
42 Ph. Niedermann, W. Hänni, N. Blanc, R. Christoph and J. Burger, *J. Vac. Sci. Technol., A*, 1996, **14**(3), 1233–1236.
43 E. Oesterschulze, W. Scholz, Ch. Mihalcea, D. Albert, B. Sobich and W. Kulisch, *Appl. Phys. Lett.*, 1997, **70**(4), 435–437.
44 E.-L. Florin, V. T. Moy and H. E. Gaub, *Science*, 1994, **264**, 415–417.
45 V. T. Moy, E.-L. Florin and H. E. Gaub, *Colloids Surf., A*, 1994, **93**, 343–348.
46 O. Livnah, E. A. Bayer, M. Wilchek and J. L. Sussman, *Proc. Natl. Acad. Sci. U. S. A.*, 1993, **90**, 5076–5080.
47 C. Yuan, A. Chen, P. Kolb and V. T. Moy, *Biochemistry*, 2000, **39**, 10219–10223.
48 For a review on the adsorption of proteins onto surfaces, see: W. Norde, *Adv. Colloid Interface Sci.*, 1986, **26**, 267–340.
49 C. Jérôme, S. Gabriel, S. Voccia, C. Detrembleur, M. Ignatova, R. Gouttebaron and R. Jérôme, *Chem. Commun.*, 2003, 2500–2501.
50 G. Lécayon, Y. Bouizem, C. Le Gressus, C. Reynaud, C. Boiziau and C. Juret, *Chem. Phys. Lett.*, 1982, **91**(6), 506–510.
51 C. Jérôme, N. Willet, R. Jérôme and A.-S. Duwez, *ChemPhysChem*, 2004, **5**, 147–149.
52 P. Silberzan, L. Léger, D. Ausserré and J. J. Benattar, *Langmuir*, 1991, **7**, 1647–1651.
53 T. Ito, M. Namba, P. Bühlmann and Y. Umezawa, *Langmuir*, 1997, **13**(16), 4323–4332.
54 T. Ito, D. Citterio, P. Bühlmann and Y. Umezawa, *Langmuir*, 1999, **15**(8), 2788–2793.
55 G. Li, N. Xi and D. H. Wang, *Nanomedicine*, 2005, **1**, 306–312.
56 L. Netzer and J. Savig, *J. Am. Chem. Soc.*, 1983, **105**, 674–676.
57 S. R. Wasserman, Y.-T. Tao and G. M. Whitesides, *Langmuir*, 1989, **5**, 1074–1087.
58 C. K. Riener, C. M. Stroh, A. Ebner, C. Klampfl, A. A. Gall, C. Romanin, Y. L. Lyubchenko, P. Hinterdorfer and H. J. Gruber, *Anal. Chim. Acta*, 2003, **479**, 59–75.
59 R. Ros, F. Schwesinger, D. Anselmetti, M. Kubon, R. Schäfer, A. Plückthun and L. Tiefenauer, *Proc. Natl. Acad. Sci. U. S. A.*, 1998, **95**, 7402–7405.
60 A. Vinckier, I. Heyvaert, A. D'Hoore, T. McKittrick, C. Van Haesendonck, Y. Engelborghs and L. Hellemans, *Ultramicroscopy*, 1995, **57**, 337–343.
61 S. Allen, X. Chen, J. Davies, M. C. Davies, A. C. Dawkes, J. C. Edwards, C. J. Roberts, J. Sefton, S. J. B. Tendler and P. M. Williams, *Biochemistry*, 1997, **36**, 7457–7463.
62 A. Ulman, *Chem. Rev.*, 1996, **96**, 1533–1554.
63 J. M. Buriak, *Chem. Rev.*, 2002, **102**(5), 1271–1308.
64 A. B. Sieval, V. Vleeming, H. Zuilhof and E. J. R. Sudhölter, *Langmuir*, 1999, **15**, 8288–8291.
65 M. R. Linford, P. Fenter, P. M. Eisenberger and C. E. D. Chidsey, *J. Am. Chem. Soc.*, 1995, **117**, 3145–3155.
66 C.-M. Yam, Z. Xiao, J. Gu, S. Boutet and C. Cai, *J. Am. Chem. Soc.*, 2003, **125**, 748–7499.
67 C. D. Bain, E. B. Troughton, Y.-T. Tao, J. Evall, G. M. Whitesides and R. G. Nuzzo, *J. Am. Chem. Soc.*, 1989, **111**(1), 321–335.
68 H. Skulason and C. D. Frisbie, *J. Am. Chem. Soc.*, 2000, **122**, 9750–9760.
69 L. A. Wenzler, G. L. Moyes, L. G. Olson, J. M. Harris and T. P. Beebe, Jr, *Anal. Chem.*, 1997, **69**, 2855–2861.
70 C. D. Frisbie, L. F. Rozsnyai, A. Noy, M. S. Wrighton and C. M. Lieber, *Science*, 1994, **265**, 2071–2074.
71 E. W. van der Vegte and G. Hadziioannou, *J. Phys. Chem. B*, 1997, **101**, 9563–9569.
72 S. Kado and K. Kimura, *Chem. Lett.*, 2001, 630–631.
73 R. Gil, J.-C. Fiaud, J.-C. Poulin and E. Schulz, *Chem. Commun.*, 2003, 2234–2235.
74 C. Nakamura, S. Takeda, M. Kageshima, M. Ito, N. Sugimoto, K. Sekizawa and J. Miyake, *Biopolymers*, 2004, **76**, 48–54.
75 H. Skulason and C. D. Frisbie, *Anal. Chem.*, 2002, **74**, 3096–3104.
76 H. Skulason and C. D. Frisbie, *J. Am. Chem. Soc.*, 2002, **124**, 15125–15133.
77 H. Schönherr, M. W. J. Beulen, J. Bügler, J. Huskens, F. C. J. M. Van Veggel, D. N. Reinhoudt and G. J. Vansco, *J. Am. Chem. Soc.*, 2000, **122**, 4963–4967.
78 T. Auletta, M. R. de Jong, A. Mulder, F. C. J. M. van Veggel, J. Huskens, D. N. Reinhoudt, S. Zou, S. Zapotoczny, H. Schönherr, G. J. Vansco and L. Kuipers, *J. Am. Chem. Soc.*, 2004, **126**, 1577–1584.
79 K. L. Johnson, K. Kendall and A. D. Roberts, *Proc. R. Soc. London, Ser. A*, 1971, **324**, 301–313.
80 L. Schmitt, M. Ludwig, H. E. Gaub and R. Tampé, *Biophys. J.*, 2000, **78**, 3275–3285.
81 A. Berquand, N. Xia, D. G. Castner, B. H. Clare, N. L. Abbott, V. Dupres, Y. Adriaensen and Y. F. Dufrêne, *Langmuir*, 2005, **21**, 5517–5523.
82 J. Gu, Z. Xiao, C.-M. Yam, G. Qin, M. Deluge, S. Boutet and C. Cai, *Biophys. J.: Biophys. Lett.*, 2005, 31–33.
83 P. Hinterdorfer, K. Schilcher, W. Baumgartner, H. J. Gruber and H. Schindler, *Nanobiology*, 1998, **4**, 39–50.
84 P. Hinterdorfer, W. Baumgartner, H. J. Gruber, K. Schilcher and H. Schindler, *Proc. Natl. Acad. Sci. U. S. A.*, 1996, **93**, 3477–3481.
85 J. K. Stuart and V. Hlady, *Langmuir*, 1995, **11**, 1368–1374.
86 P. Hinterdorfer, F. Kienberger, A. Raab, H. J. Gruber, W. Baumgartner, G. Kada, C. Riener, S. Wielert-Badt, C. Borken and H. Schindler, *Single Mol.*, 2000, **1**(2), 99–103.
87 C. K. Riener, C. M. Stroh, A. Ebner, C. Klampfl, A. A. Gall, C. Romanin, Y. L. Lyubchenko, P. Hinterdorfer and H. J. Gruber, *Anal. Chim. Acta*, 2003, **497**, 101–114.
88 T. Haselgrübler, A. Amerstorfer, H. Schindler and H. J. Gruber, *Bioconjugate Chem.*, 1995, **6**, 242–248.
89 F. Kienberger, A. Ebner, H. J. Gruber and P. Hinterdorfer, *Acc. Chem. Res.*, 2006, **39**, 29–36.
90 R. Gabai, L. Segev and E. Joselevich, *J. Am. Chem. Soc.*, 2005, **127**, 11390–11398.
91 F. Kienberger, G. Kada, H. J. Gruber, V. P. Pastushenko, C. Riener, M. Trieb, H.-G. Knaus, H. Schindler and P. Hinterdorfer, *Single Mol.*, 2000, **1**(1), 59–65.
92 A. Raab, W. Han, D. Badt, S. J. Smith-Gill, S. M. Lindsay, H. Schindler and P. Hinterdorfer, *Nat. Biotechnol.*, 1999, **17**, 902–905.

93 A. Ebner, F. Kienberger, G. Kada, C. M. Stroh, M. Geretschläger, A. S. M. Kamruzzahan, L. Wildling, W. T. Lindsay, H. J. Gruber and P. Hinterdorfer, *ChemPhysChem*, 2005, **6**, 897–900.
94 C. Stroh, H. Wang, R. Bash, B. Ashcroft, J. Nelson, H. Gruber, D. Lohr, S. M. Lindsay and P. Hinterdorfer, *Proc. Natl. Acad. Sci. U. S. A.*, 2004, **101**(34), 12503–12507.
95 C. Stroh, A. Ebner, M. Geretschläger, G. Freudenthaler, F. Kienberger, A. S. M. Kamruzzahan, S. J. Smith-Gill, H. J. Gruber and P. Hinterdorfer, *Biophys. J.*, 2004, **87**, 1981–1990.
96 A. T. Woolley, C. L. Cheung, J. H. Hafner and C. M. Lieber, *Chem. Biol.*, 2000, **7**, 193–204.
97 J. H. Hafner, C.-L. Cheung, A. T. Wooley and C. M. Lieber, *Prog. Biophys. Mol. Biol.*, 2001, **77**, 73–110.
98 H. Dai, J. H. Hafner, A. G. Rinzler, D. T. Colbert and R. E. Smalley, *Nature*, 1996, **384**, 147–150.
99 H. Nishijima, S. Kamo, S. Akita and Y. Nakayama, *Appl. Phys. Lett.*, 1999, **74**(26), 4061–4063.
100 J. H. Hafner, C. L. Cheung and C. M. Lieber, *Nature*, 1999, **398**, 761–762.
101 C. L. Cheung, J. H. Hafner and C. M. Lieber, *Proc. Natl. Acad. Sci. U. S. A.*, 2000, **97**(8), 3809–3813.
102 J. H. Hafner, C. L. Cheung and C. M. Lieber, *J. Am. Chem. Soc.*, 1999, **121**, 9750–9751.
103 H. Hiura, T. W. Ebbesen and K. Tanigaki, *Adv. Mater.*, 1995, **7**(3), 275–276.
104 Y. Yang, J. Zhang, X. Nan and Z. Liu, *J. Phys. Chem. B*, 2002, **106**, 4139–4144.
105 S. S. Wong, A. T. Woolley, T. W. Odom, J.-L. Huang, P. Kim, D. V. Vezenov and C. M. Lieber, *Appl. Phys. Lett.*, 1998, **73**(23), 3465–3467.
106 L. Chen, K. A. Haushalter, C. M. Lieber and G. L. Verdine, *Chem. Biol.*, 2002, **9**, 345–350.
107 L. Chen, C. L. Cheung, P. D. Ashby and C. M. Lieber, *Nano Lett.*, 2004, **4**(9), 1725–1731.
108 S. S. Wong, E. Joselevich, A. T. Woolley, C. L. Cheung and C. M. Lieber, *Nature*, 1998, **394**, 52–55.
109 S. S. Wong, A. T. Woolley, E. Joselevich, C. L. Cheung and C. M. Lieber, *J. Am. Chem. Soc.*, 1998, **120**, 8557–8558.

